basic residues available for intermolecular interactions with ligands, including association with the negatively-charged sugar-phosphate backbone of dsRNA. MSR1 bound to acetylated LDL is internalized through receptor-mediated endocytosis, dissociating under acidic conditions within the endosome due to the loss of ion pairing between Glu^{337} and the conserved Lys residues within the collagen-like domain [34,42]. We presume that MSR1 functions similarly in the uptake of dsRNA from the extracellular milieu. This may explain why inhibitors of endosomal acidification block TLR3-mediated antiviral responses, as we have shown previously for Huh7.5-TLR3 cells [4], and inhibit the co-immunoprecipitation of HCV RNA with TLR3 in infected Huh7.5-TLR3 cells (Fig. 6D).

An important observation to emerge from these studies is that hepatocytes are capable of sensing HCV infection in adjacent cells, and that MSR1 mediates this response by acting as a carrier of replication intermediates (presumably dsRNA) from the extracellular milieu to endosomally expressed TLR in uninfected cells. While it is often assumed that TLR3 expressed within parenchymal cells such as hepatocytes may sense virus infection in neighboring cells, we demonstrated this formally in co-cultures of HCV-nonpermissive, TLR3-competent cells (293FT or PH5CH8 cells) and infected Huh-7.5 cells that are deficient in both TLR3 and RIG-I sensing of HCV infection [17,26] (Figs. 6 and 7). We show that this results in a localized antiviral effect, restricting the replication of virus in the co-cultured cells, and that it is dependent upon MSR1 expression in the uninfected cells since it can be blocked by RNAi-mediated depletion of MSR1 (Fig. 7B).

These observations have important implications for the pathogenesis of chronic hepatitis C. For reasons that are unclear, only a small fraction of hepatocytes appear to be infected with HCV in these patients [25]. Two-photon immunofluorescence microscopy of frozen sections of infected human liver tissue has revealed clusters of infected cells, identified either by detection of HCV-specific antigens or dsRNA replication intermediates, typically surrounded by greater numbers of uninfected cells [25]. The presence of these discreet foci of infection suggests that the spread of virus is actively restricted within the liver. The data we present here suggest a model in which TLR3 mediates the establishment of an antiviral state in uninfected cells adjacent to those that are infected in a process that is facilitated by the dsRNA-scavenging actions of MSR1. Such a model also explains why HCV infection induces ISG expression within the liver, despite its ability to disrupt both RIG-I and TLR3 responses by NS3/4A-mediated cleavage of the RIG-I adaptor molecule, MAVS [15,16], and the TLR3 adaptor molecule, TICAM-1 (TRIF), within infected cells [4,18]. TLR3 sensing of HCV infection is not likely to be restricted to neighboring hepatocytes, as we have demonstrated here, but may also occur in tissue-resident macrophages (Kupffer cells) or monocyte-macrophages recruited to the site of infection. TLR7 expressed within plasmacytoid dendritic cells (pDCs) may also sense infection in other cells [43]. While less robust on a single cell level than in these "professional" innate immune cells, TLR3-mediated antiviral responses in the very large number of parenchymal hepatocytes exposed to HCV may nonetheless make a substantial contribution overall to the induction of intrahepatic ISG responses observed in patients with chronic hepatitis C [24].

Materials and Methods

Cells

Huh-7.5 cells [44] were a gift from Charles Rice (Rockefeller University, NY). Huh-7.5 cells engineered to express either TLR3 or the TLR3 mutants ΔTIR, H539E or N541A have been described previously [4]. 293FT cells, human embryonic kidney cells transformed with SV40 T antigen, were purchased from Invitrogen (Carlsbad, CA). 293-hTLR3 cells (engineered to over-express human TLR3) were purchased from InvivoGen. The non-neoplastic T-antigen immortalized hepatocyte cell line PH5CH8 has been described previously [30,45]. These cells were cultured in Dulbecco's modified Eagle's medium (Invitrogen) supplemented with 10% fetal bovine serum. Blasticidin (2 μg/ml) or G418 (0.3 mg/ml) was added for the selection of cells exogenously expressing TLR3-Flag, Myc-MSR1 and related mutants. G418 (0.3 mg/ml) was added for the selection of HCV RNA replicon colonies.

Virus

Two strains of HCV were used in these studies: the genotype 2a JFH-1 virus [46], and HJ3-5, a cell culture-adapted genotype 1a/2a chimeric virus containing the structural proteins of the genotype 1a H77 virus placed within the background of JFH-1 virus [47,48]. HJ3-5/GLuc2A is a derivative of HJ3-5 containing the *Gaussia princeps* luciferase (GLuc) coding sequence fused to the foot-and-mouth disease virus (FMDV) 2A sequence and inserted between p7 and NS2 of HJ3-5 virus [49]. Cells were infected at an m.o.i. of 1. GLuc activity in supernatants was measured by BioLux *Gaussia* Luciferase Assay Kit (New England Biolabs, Ipswich, MA) using a Synergy2 multi-mode microplate reader (BioTek, Winooski, VT). HJ3-5/5A-YFP is another derivative of HJ3-5 containing yellow fluorescent protein (YFP) coding sequence fused to NS5A sequence [35].

Plasmids

ptat2ANeoH77S [27] contains the *tat* protein, 15 amino acids of the FMDV 2A protein and neomycin phosphotransferase (Neo^R) downstream of HCV internal ribosome entry site (IRES) and the full-length H77S (genotype 1a) polyprotein-coding sequence downstream of the encephalomyocarditis virus IRES. pIFN-β-Luc and pPRDII-Luc have been described previously [50,51]. pIFN-β-mCherry, which expresses the mCherry fluorescent protein under transcriptional control of the IFN-β promoter, was constructed by replacing the firefly luciferase sequence in pIFN-β-Luc with the mCherry sequence. pJFH1-T3 was constructed by introducing a T3 promoter downstream of the HCV 3′UTR in pJFH1 [46].

pCX4neo/Myc-MSR1 and pCX4bsr/Myc-MSR1 were constructed from the retroviral vectors pCX4neo and pCX4br [52], which contain the resistance gene for neomycin and blasticidin respectively. A DNA fragment encoding MSR1 (accession no. NM_138715) was amplified from cDNA obtained from Huh-7 cell DNA by PCR using PrimeSTAR HS DNA polymerase (TaKaRa) and primers with *Sph*I (forward) and the *Not*I (reverse) recognition sites that were designed to enable expression of the MSR1 ORF. The DNA was cloned into the *Sph*I and *Not*I sites of pCX4neo/Myc and pCX4bsr/Myc, fusing MSR1 sequence to Myc. Mutations within the Myc-MSR1 sequence were subsequently constructed by PCR mutagenesis as previously described [53]. The nucleotide sequences of these vectors were confirmed by DNA sequencing. Cells stably expressing Myc-MSR1 were prepared as previously described [54].

Synthetic HCV dsRNA

pJFH1-T3 was linearized by either *Xba*I or *Eco*RI to provide templates for synthesis of positive- or negative-stranded HCV RNA using T7 or T3 MEGAscript kits (Ambion, Austin, TX). Positive- and negative-stranded HCV RNA products were

annealed to produce dsRNA by heating at 70°C for 10 minutes followed by slow cooling to room temperature. The annealed product was assayed for sensitivity to S1 nuclease (Promega, Madison, WI) to confirm that it was double-stranded.

Poly(I:C)

High molecular weight (HMW) poly(I:C) was purchased from Invivogen (San Diego, CA). Cells were exposed to a concentration of 50 μg/ml for 6 hrs unless otherwise stated. Fluorescein-labeled HMW poly(I:C) (Invivogen) was used to monitor dsRNA uptake by cells. Cells were mock-exposed or exposed to 10 μg/ml fluorescein-labeled poly (I:C) for 8, 16 or 24 hrs, then harvested by trypsinization, washed twice in phosphate buffered saline (PBS) and fixed for 15 minutes in 4% paraformaldehyde. After additional washing in 1× PBS, the fluorescence intensity of cell populations was analyzed using a Beckman Coulter (Dako) CyAn flow cytometer.

Promoter reporter assays

IFN-β and NF-κB-dependent promoter activities were assayed using firefly luciferase reporters, pIFN-β-Luc or pPRDII-Luc, with the reporter plasmid pRL-CMV used as an internal control for transfection efficiency as previously described [55]. A Turner Designs Luminometer Model TD-20/20 (Promega, Madison, WI) was used to measure luciferase activity. Data shown represent means ± s.d. from three independent transfection experiments.

Immunoblot analysis

Preparation of cell lysates and SDS-PAGE were carried out as previously described [56]. Total protein was transferred to Immobilon-psq PVDF membranes (Millipore, Billerica, MA) using a Trans-blot SD semi-dry transfer cell (Bio-Rad, Hercules, CA). Primary antibodies included anti-Flag (M2; Sigma, St Louis, MO), anti-Myc (9B11; Cell Signaling, Danvers, MA), anti-ISG15 (H-150; Santa Cruz Biotechnology Inc., Santa Cruz, CA), anti-MSR1 (H-190; Santa Cruz Biotechnology Inc.), and anti-β-actin antibody (AC-15; Sigma). Secondary antibodies were IRDye-conjugated anti-mouse IgG and anti-rabbit IgG (LI-COR Biosciences, Lincoln, NE). Immunocomplexes were detected with an Odyssey infrared imaging system (LI-COR Biosciences).

Quantitative RT-PCR analysis

Total cellular RNA was isolated using the RNeasy mini kit (Qiagen, Valencia, CA). The iScript one-step RT-PCR kit with SYBR Green and CFX96 real-time system (Bio-Rad) were used to quantify the abundance of IFN-β, ISG56, GAPDH mRNA or HCV RNA. We used the following forward and reverse primer sets: IFN-β, 5′-GTGCCTGGACCATAGTCAGAGTGG-3′ (forward), 5′-TGTCCAGTCCCAGAGGCACAGG-3′ (reverse); ISG56, AAGCTTGAGCCTCCTTGGGTTCGT-3′ (forward), 5′-TCAAAGTCAGCAGCCAGTCTCAGG-3′ (reverse); GAPDH [53], HCV, 5′-CATGGCGTTAGTATGAGTGTCGT-3′ (forward), 5′-CCCTATCAGGCAGTACCACAA-3′ (reverse). IFN-β, ISG56 and HCV RNAs were normalized to GAPDH mRNA. Results shown represent means ± s.d. from three independent experiments.

Co-immunoprecipitation of Flag-TLR3 or Myc-MSR1 with HCV RNA

Total cell lysates were prepared using lysis buffer (PBS containing 0.2% Triton X-100, RNase inhibitor and protease inhibitor cocktail), followed by immunoprecipitation with anti-Flag or anti-Myc antibodies using protein G sepharose (GE healthcare). RNAs were extracted from the immunoprecipitates using Trizol (Invitrogen), and assayed for HCV RNA by RT-PCR using the Superscript III One-step RT-PCR system (Invitrogen) followed by agarose gel electrophoresis.

MSR1-depleted cells and Myc-MSR1 expression

Short hairpin RNA (shRNA) targeting MSR1 (shMSR1, 5′-GCATTGATGAGAGTGCTATTG-3′) or non-targeting control shRNA (Sigma; Mission shRNA SHC-002) were introduced into Huh7.5-TLR3 or PH5CH8 cells by lentiviral transfer. MSR1-depleted Huh7.5-TLR3/shMSR1 and PH5CH8/shMSR1 and related control cells, Huh7.5-TLR3/shNT or PH5CH8/shNT cells, were selected by addition of puromycin (5 μg/ml) to the cell culture medium. MSR1 expression was reconstituted in MSR1-depleted cells by retroviral transfer of the Myc-MSR1 sequence in pCX4neo Myc-MSR1, which lacks the shMSR1 target sequence within the 5′UTR of MSR1 mRNA [57]. Cells stably expressing Myc-MSR1 were selected by growth in G418 (0.3 mg/ml).

For analysis of the RNA-binding domain in MSR1, pCX4neo-Myc-MSR1 was subjected to PCR-based mutagenesis using standard methods, with the sequence of the manipulated regions of the plasmid confirmed by DNA sequencing. Cell surface expression of MSR1 and related mutants was analyzed by flow cytometry. MSR1 has a transmembrane domain between aa 51–73, with its carboxyl terminus exposed to the extracellular environment. For detection of MSR1 on the cell surface, non-permeabilized cells were fixed with 2% paraformaldehyde followed by incubation with anti-MSR1 antibody (Santacruz, H-190) for 1 h at room temperature. Cells were washed three times with PBS, and incubated with R-phycoerythrin-conjugated anti-rabbit IgG secondary antibody (Jackson ImmunoResearch) for 30 min at room temperature. Fluorescent intensity of cells was determined using a FACScan (Becton Dickinson) flow cytometer.

Measurements of apoptosis in infected cells

Huh-7.5 cells were infected with HJ3-5/GLuc2A virus at an m.o.i. of 0.03, or mock-infected, and cultured for 4 days. As a positive control, cells were treated with 1 μM staurosporine for 6 hrs. Cells were harvested by trypsinization, washed twice in PBS and fixed in 4% paraformaldehyde, then stained for cleaved caspase 3 and HCV core protein as described previously [37]. DNA fragmentation was analyzed by terminal deoxynucleotidyl-transferase-mediated dUTP-biotin nick end-labeling (TUNEL) system (Promega, Madison, WI). Positive cells were quantified by flow cytometry as described previously [37].

Statistical methods

Statistical comparisons were carried out using Student's T test unless otherwise noted. Calculations were made with Excel 2008 for Mac (Microsoft) or Prism V for Mac OS X (GraphPad Software).

Supporting Information

Figure S1 Replicon colony formation assay demonstrates that TLR3 expression restricts HCV replication. Ten μg RNA, synthesized in vitro from linearized ptat2AneoH77S DNA using a T7 MEGAscript kit (Ambion), were electroporated into Huh7.5-TLR3, -ΔTIR, -H539E or -N541A cells in a 4-mm cuvette by pulsing once at 400 V, 250 μF, and infinite Ω in a BioRad Gene Pulser Xcell apparatus. The cells were then cultured in G418 (0.3 mg/ml) for 3 weeks, and surviving cell colonies stained with Coomassie brilliant blue (0.06% in 50% methanol-10% acetic acid).
(TIF)

Figure S2 TLR3 preferentially senses very high molecular weight poly(I:C). (**A**) To determine whether TLR3 discriminates between dsRNA of different lengths corresponding to the size of viral genomes, we studied two dsRNA surrogates, low-molecular weight (LMW) and high-molecular weight (HMW) poly(I:C), that are between 0.2–1.0 and 1.5–8 kilobase pairs, respectively. (**B**) Both LMW and HMW poly(I:C) stimulated IFN-β promoter activity in a dose-dependent manner when added to the medium bathing (left) Huh-7.5 cells engineered to express wt TLR3 (Huh7.5-TLR3 cells), but not (right) Huh7.5-ΔTIR cells that express a defective TLR3 lacking the TIR domain and thus incapable of signaling. Importantly, however, HMW poly(I:C) was 300-fold more active than LMW poly(I:C) on a molar basis in stimulating IFN-β promoter activity. (**C**) This was reflected in significantly greater induction of ISG56 mRNA expression by HMW vs. LMW poly(I:C) in Huh7.5-TLR3 cells or PH5CH8 cells that naturally express TLR3. (**D**) At comparable concentrations, HMW poly(I:C) was also more active than LMW poly(I:C) in stimulating ISG15 protein expression in Huh7.5-TLR3 cells. Note the absence of ISG15 expression induced by either poly(I:C) in Huh7.5-H539E cells that express an inactive TLR3 mutant that is defective in dsRNA binding. (**E**) Similar differences in poly(I:C) induction of ISG15 protein expression were observed in PH5CH8 cells. Note that ISG15 expression was reduced by shRNA knockdown of TLR3 in these cells. Collectively, these results suggest that very lengthy dsRNA, such as viral replication intermediates, are more powerful inducers of TLR3-mediated antiviral responses than dsRNAs under 1 kb in length. While the mechanistic basis of this is uncertain, one possibility is that the greater signaling strength derives from progressive recruitment of multiple TLR3 ectodomains aligned along a single dsRNA molecule.
(TIF)

Figure S3 Induction of IFN-β promoter activity in 293-hTLR3/IFN-β-mCherry cells co-cultured with HCV-infected Huh-7.5 cells. (**A**) Human 293-hTLR3/IFN-β-mCherry cells transduced to overexpress TLR3 and the IFN-β-mCherry reporter were co-cultured with infected or uninfected Huh-7.5 cells using the same general experimental design as in the experiment shown in Fig. 6A in the main manuscript. (**B**) Immunofluorescence microscopy demonstrating induction of mCherry expression in 293-hTLR3/IFN-β-mCherry + Huh-7.5 cell co-cultures upon stimulation with poly(I:C) or infection with HJ3-5/NS5A-YFP virus. HCV replication was visualized by YFP expression and is observed in cells adjacent to those expressing mCherry in the two-color merged images at the bottom. Nuclei were visualized by DAPI counterstain.
(TIF)

Figure S4 Absence of apoptosis in HJ3-5/GLuc2A-infected cells. Analysis of cleaved caspase 3 and HCV core protein (top row) and DNA fragmentation by TUNEL assay (bottom row) in Huh-7.5 cells at 4 d following mock infection or infection with HJ3-5/GLuc2A virus at a m.o.i. of 0.03. Cells treated with 1 μM staurosporine for 3 hrs are shown as a positive control for apoptosis induction.
(TIF)

Acknowledgments

The authors are grateful to Zongdi Feng for helpful advice and review of the manuscript, and to Cindy Hensley for expert technical assistance.

Author Contributions

Conceived and designed the experiments: HD DY CW DRM FH SML. Performed the experiments: HD DY DRM FH. Analyzed the data: HD DY DRM CW SML. Contributed reagents/materials/analysis tools: NK. Wrote the paper: HD DRM SML.

References

1. Lemon SM, Walker C, Alter MJ, Yi M (2007) Hepatitis C viruses. In: Knipe DM, Howley PM, Griffin DE, Martin MA, Lamb RA, et al., editors. Fields Virology, 5th Ed. Philadelphia: Lippincott Williams & Wilkins. pp. 1253–1304.
2. Lemon SM (2010) Induction and evasion of innate antiviral responses by hepatitis C virus. J Biol Chem 285: 22741–22747.
3. Yoneyama M, Kikuchi M, Natsukawa T, Shinobu N, Imaizumi T, et al. (2004) The RNA helicase RIG-I has an essential function in double-stranded RNA-induced innate antiviral responses. Nat Immunol 5: 730–737.
4. Wang N, Liang Y, Devaraj S, Wang J, Lemon SM, et al. (2009) Toll-like receptor 3 mediates establishment of an antiviral state against hepatitis C virus in hepatoma cells. J Virol 83: 9824–9834.
5. Kato H, Takeuchi O, Sato S, Yoneyama M, Yamamoto M, et al. (2006) Differential roles of MDA5 and RIG-I helicases in the recognition of RNA viruses. Nature 441: 101–105.
6. Alexopoulou L, Holt AC, Medzhitov R, Flavell RA (2001) Recognition of double-stranded RNA and activation of NF-kappaB by Toll-like receptor 3. Nature 413: 732–738.
7. Kawai T, Akira S (2011) Toll-like receptors and their crosstalk with other innate receptors in infection and immunity. Immunity 34: 637–650.
8. Hornung V, Ellegast J, Kim S, Brzozka K, Jung A, et al. (2006) 5′-Triphosphate RNA is the ligand for RIG-I. Science 314: 994–997.
9. Vercammen E, Staal J, Beyaert R (2008) Sensing of viral infection and activation of innate immunity by toll-like receptor 3. Clin Microbiol Rev 21: 13–25.
10. Xagorari A, Chlichlia K (2008) Toll-like receptors and viruses: induction of innate antiviral immune responses. Open Microbiol J 2: 49–59.
11. Johnsen IB, Nguyen TT, Ringdal M, Tryggestad AM, Bakke O, et al. (2006) Toll-like receptor 3 associates with c-Src tyrosine kinase on endosomes to initiate antiviral signaling. EMBO J 25: 3335–3346.
12. de Bouteiller O, Merck E, Hasan UA, Hubac S, Benguigui B, et al. (2005) Recognition of double-stranded RNA by human toll-like receptor 3 and downstream receptor signaling requires multimerization and an acidic pH. J Biol Chem 280: 38133–38145.
13. Saito T, Owen DM, Jiang F, Marcotrigiano J, Gale M, Jr. (2008) Innate immunity induced by composition-dependent RIG-I recognition of hepatitis C virus RNA. Nature 454: 523–527.
14. Loo YM, Owen DM, Li K, Erickson AL, Johnson CL, et al. (2006) Viral and therpeutic control of interferon beta promoter stimulator 1 during hepatitis C virus infection. ProcNatlAcadSci USA 103: 6001–6006.
15. Meylan E, Curran J, Hofmann K, Moradpour D, Binder M, et al. (2005) Cardif is an adaptor protein in the RIG-I antiviral pathway and is targeted by hepatitis C virus. Nature 437: 1167–1172.
16. Li XD, Sun L, Seth RB, Pineda G, Chen ZJ (2005) Hepatitis C virus protease NS3/4A cleaves mitochondrial antiviral signaling protein off the mitochondria to evade innate immunity. ProcNatlAcadSci USA 102: 17717–17722.
17. Li K, Chen Z, Kato N, Gale M, Jr., Lemon SM (2005) Distinct poly-I:C and virus-activated interferon signaling pathways in hepatocytes. J BiolChem 280: 16739–16747.
18. Li K, Foy E, Ferreon JC, Nakamura M, Ferreon ACM, et al. (2005) Immune evasion by hepatitis C virus NS3/4A protease-mediated cleavage of the TLR3 adaptor protein TRIF. Proc Natl Acad Sci U S A 102: 2992–2997.
19. Targett-Adams P, Boulant S, McLauchlan J (2008) Visualization of double-stranded RNA in cells supporting hepatitis C virus RNA replication. J Virol 82: 2182–2195.
20. Limmon GV, Arredouani M, McCann KL, Corn Minor RA, Kobzik L, et al. (2008) Scavenger receptor class-A is a novel cell surface receptor for double-stranded RNA. FASEB J 22: 159–167.
21. Dieudonne A, Torres D, Blanchard S, Taront S, Jeannin P, et al. (2012) Scavenger receptors in human airway epithelial cells: role in response to double-stranded RNA. PLoS One 7: e41952.
22. DeWitte-Orr SJ, Collins SE, Bauer CM, Bowdish DM, Mossman KL An accessory to the 'Trinity': SR-As are essential pathogen sensors of extracellular dsRNA, mediating entry and leading to subsequent type I IFN responses. PLoS Pathog 6: e1000829.
23. Yamashita M, Chattopadhyay S, Fensterl V, Saikia P, Wetzel JL, et al. (2012) Epidermal growth factor receptor is essential for toll-like receptor 3 signaling. Sci Signal 5: ra50.
24. Sarasin-Filipowicz M, Oakeley EJ, Duong FH, Christen V, Terracciano L, et al. (2008) Interferon signaling and treatment outcome in chronic hepatitis C. Proc Natl Acad Sci U S A 105: 7034–7039.
25. Liang Y, Shilagard T, Xiao SY, Snyder N, Lau D, et al. (2009) Visualizing hepatitis C virus infections in human liver by two-photon microscopy. Gastroenterology 137: 1448–1458.

26. Sumpter R, Jr., Loo YM, Foy E, Li K, Yoneyama M, et al. (2005) Regulating intracellular antiviral defense and permissiveness to hepatitis C virus RNA replication through a cellular RNA helicase, RIG-I. J Virol 79: 2689–2699.
27. Yi M, Lemon SM (2004) Adaptive mutations producing efficient replication of genotype 1a hepatitis C virus RNA in normal Huh7 cells. J Virol 78: 7904–7915.
28. Li K, Li NL, Wei D, Pfeffer SR, Fan M, et al. (2012) Activation of chemokine and inflammatory cytokine response in hepatitis C virus-infected hepatocytes depends on Toll-like receptor 3 sensing of hepatitis C virus double-stranded RNA intermediates. Hepatology 55: 666–675.
29. Tuplin A, Evans DJ, Simmonds P (2004) Detailed mapping of RNA secondary structures in core and NS5B-encoding region sequences of hepatitis C virus by RNase cleavage and novel bioinformatic prediction methods. J GenVirol 85: 3037–3047.
30. Kato N, Ikeda M, Mizutani T, Sugiyama K, Noguchi M, et al. (1996) Replication of hepatitis C virus in cultured non-neoplastic human hepatocytes. Japanese Journal of Cancer Research (Amsterdam) 87: 787–792.
31. Leonard JN, Ghirlando R, Askins J, Bell JK, Margulies DH, et al. (2008) The TLR3 signaling complex forms by cooperative receptor dimerization. Proc Natl Acad Sci U S A 105: 258–263.
32. Kodama T, Freeman M, Rohrer L, Zabrecky J, Matsudaira P, et al. (1990) Type I macrophage scavenger receptor contains alpha-helical and collagen-like coiled coils. Nature 343: 531–535.
33. Shimakami T, Yamane D, Jangra RK, Kempf BJ, Spaniel C, et al. (2012) Stabilization of hepatitis C RNA by an Ago2-miR-122 complex. Proc Natl Acad Sci U S A 109: 941–946.
34. Anachi RB, Siegel DL, Baum J, Brodsky B (1995) Acid destabilization of a triple-helical peptide model of the macrophage scavenger receptor. FEBS Lett 368: 551–555.
35. Ma Y, Anantpadma M, Timpe JM, Shanmugam S, Singh SM, et al. (2011) Hepatitis C virus NS2 protein serves as a scaffold for virus assembly by interacting with both structural and nonstructural proteins. J Virol 85: 86–97.
36. Li Y, Masaki T, Yamane D, McGivern DR, Lemon SM (2013) Competing and noncompeting activities of miR-122 and the 5′ exonuclease Xrn1 in regulation of hepatitis C virus replication. Proc Natl Acad Sci U S A 110: 1881–1886.
37. Kannan RP, Hensley LL, Evers L, Lemon SM, McGivern DR (2011) Hepatitis C virus infection causes cell cycle arrest at the level of entry to mitosis. J Virol 85: 7989–8001.
38. Suzuki H, Kurihara Y, Takeya M, Kamada N, Kataoka M, et al. (1997) A role for macrophage scavenger receptors in atherosclerosis and susceptibility to infection. Nature 386: 292–296.
39. Yew KH, Carsten B, Harrison C (2010) Scavenger receptor A1 is required for sensing HCMV by endosomal TLR-3/-9 in monocytic THP-1 cells. Mol Immunol 47: 883–893.
40. Freeman M, Ashkenas J, Rees DJ, Kingsley DM, Copeland NG, et al. (1990) An ancient, highly conserved family of cysteine-rich protein domains revealed by cloning type I and type II murine macrophage scavenger receptors. Proc Natl Acad Sci U S A 87: 8810–8814.
41. Doi T, Higashino K, Kurihara Y, Wada Y, Miyazaki T, et al. (1993) Charged collagen structure mediates the recognition of negatively charged macromolecules by macrophage scavenger receptors. J Biol Chem 268: 2126–2133.
42. Doi T, Kurasawa M, Higashino K, Imanishi T, Mori T, et al. (1994) The histidine interruption of an alpha-helical coiled coil allosterically mediates a pH-dependent ligand dissociation from macrophage scavenger receptors. J Biol Chem 269: 25598–25604.
43. Takahashi K, Asabe S, Wieland S, Garaigorta U, Gastaminza P, et al. (2010) Plasmacytoid dendritic cells sense hepatitis C virus-infected cells, produce interferon, and inhibit infection. Proc Natl Acad Sci U S A 107: 7625–7626.
44. Blight KJ, McKeating JA, Rice CM (2002) Highly permissive cell lines for subgenomic and genomic hepatitis C virus RNA replication. J Virol 76: 13001–13014.
45. Ikeda M, Sugiyama K, Mizutani T, Tanaka T, Tanaka K, et al. (1998) Human hepatocyte clonal cell lines that support persistent replication of hepatitis C virus. Virus Res 56: 157–167.
46. Wakita T, Pietschmann T, Kato T, Date T, Miyamoto M, et al. (2005) Production of infectious hepatitis C virus in tissue culture from a cloned viral genome. Nature Medicine 11: 791–796.
47. Yi M, Ma Y, Yates J, Lemon SM (2007) Compensatory mutations in E1, p7, NS2, and NS3 enhance yields of cell culture-infectious intergenotypic chimeric hepatitis C virus. J Virol 81: 629–638.
48. Ma Y, Yates J, Liang Y, Lemon SM, Yi M (2008) NS3 helicase domains involved in infectious intracellular hepatitis C virus particle assembly. J Virol 82: 7624–7639.
49. Shimakami T, Yamane D, Welsch C, Hensley L, Jangra RK, et al. (2012) Base-pairing between Hepatitis C Virus RNA and miR-122 3′ of its Seed Sequence is Essential for Genome Stabilization and Production of Infectious Virus. J Virol 86(13): 7372–7383.
50. Lin R, Genin P, Mamane Y, Hiscott J (2000) Selective DNA binding and association with the CREB binding protein coactivator contribute to differential activation of alpha/beta interferon genes by interferon regulatory factors 3 and 7. Mol Cell Biol 20: 6342–6353.
51. Fredericksen B, Akkaraju GR, Foy E, Wang C, Pflugheber J, et al. (2002) Activation of the interferon-beta promoter during hepatitis C virus RNA replication. Viral Immunol 15: 29–40.
52. Akagi T, Sasai K, Hanafusa H (2003) Refractory nature of normal human diploid fibroblasts with respect to oncogene-mediated transformation. Proc Natl Acad Sci U S A 100: 13567–13572.
53. Dansako H, Naganuma A, Nakamura T, Ikeda F, Nozaki A, et al. (2003) Differential activation of interferon-inducible genes by hepatitis C virus core protein mediated by the interferon stimulated response element. Virus Res 97: 17–30.
54. Naganuma A, Dansako H, Nakamura T, Nozaki A, Kato N (2004) Promotion of microsatellite instability by hepatitis C virus core protein in human non-neoplastic hepatocyte cells. Cancer Res 64: 1307–1314.
55. Dansako H, Ikeda M, Ariumi Y, Wakita T, Kato N (2009) Double-stranded RNA-induced interferon-beta and inflammatory cytokine production modulated by hepatitis C virus serine proteases derived from patients with hepatic diseases. Arch Virol 154: 801–810.
56. Dansako H, Naka K, Ikeda M, Kato N (2005) Hepatitis C virus proteins exhibit conflicting effects on the interferon system in human hepatocyte cells. Biochem Biophys Res Commun 336: 458–468.
57. Dansako H, Ikeda M, Kato N (2007) Limited suppression of the interferon-beta production by hepatitis C virus serine protease in cultured human hepatocytes. Febs J 274: 4161–4176.
58. Marchler-Bauer A, Lu S, Anderson JB, Chitsaz F, Derbyshire MK, et al. (2011) CDD: a Conserved Domain Database for the functional annotation of proteins. Nucleic Acids Res 39: D225–229.

HEPATOLOGY
Official Journal of the American Association for the Study of Liver Diseases

Adenosine Kinase Is a Key Determinant for the Anti-HCV Activity of Ribavirin

Kyoko Mori,[1] Osamu Hiraoka,[2] Masanori Ikeda,[1] Yasuo Ariumi,[1] Akiko Hiramoto,[3] Yusuke Wataya,[3] and Nobuyuki Kato[1]

Ribavirin (RBV) is often used in conjunction with interferon-based therapy for patients with chronic hepatitis C. There is a drastic difference in the anti–hepatitis C virus (HCV) activity of RBV between the HuH-7-derived assay system, OR6, possessing the RBV-resistant phenotype (50% effective concentration [EC_{50}]: >100 μM) and the recently discovered Li23-derived assay system, ORL8, possessing the RBV-sensitive phenotype (EC_{50}: 8 μM; clinically achievable concentration). This is because the anti-HCV activity of RBV was mediated by the inhibition of inosine monophosphate dehydrogenase in RBV-sensitive ORL8 cells harboring HCV RNA. By means of comparative analyses using RBV-resistant OR6 cells and RBV-sensitive ORL8 cells, we tried to identify host factor(s) determining the anti-HCV activity of RBV. We found that the expression of adenosine kinase (ADK) in ORL8 cells was significantly higher than that in RBV-resistant OR6 cells harboring HCV RNA. Ectopic ADK expression in OR6 cells converted them from an RBV-resistant to an RBV-sensitive phenotype, and inhibition of ADK abolished the activity of RBV. We showed that the differential ADK expression between ORL8 and OR6 cells was not the result of genetic polymorphisms in the ADK gene promoter region and was not mediated by a microRNA control mechanism. We found that the 5' untranslated region (UTR) of ADK messenger RNA in ORL8 cells was longer than that in OR6 cells, and that only a long 5' UTR possessed internal ribosome entry site (IRES) activity. Finally, we demonstrated that the long 5' UTR functioned as an IRES in primary human hepatocytes. *Conclusion*: These results indicate that ADK acts as a determinant for the activity of RBV and provide new insight into the molecular mechanism underlying differential drug sensitivity. (HEPATOLOGY 2013;58:1236-1244)

See Editorial on Page 1203

Hepatitis C virus (HCV) is an enveloped RNA virus, the genome of which consists of a positive-stranded 9.6-kilobase (kb) RNA encoding 10 structural and nonstructural (NS) proteins.[1] The combination of pegylated-interferon (Peg-IFN) and ribavirin (RBV) was the standard treatment for patients with chronic hepatitis C (CHC) until last year, when a new triple-agent combination therapy using an inhibitor of HCV NS3-4A protease (i.e., either telaprevir or boceprevir), in combination with Peg-IFN and RBV, was started.[2] The sustained virologic response (SVR) rate of genotype 1 using this new therapy is expected to increase from 55% to more than 70%.[3] However, there has also been an increase in side effects by RBV in the triple therapy, including several severe side effects, such as skin rash by telaprevir, ageusia by boceprevir, and advanced anemia by telaprevir/boceprevir.[3,4]

Abbreviations: Abs, antibodies; ADK, adenosine kinase; 5azaC, 5-azacytidine; CC_{50}, 50% cytotoxic concentration; cDNA, complementary DNA; CHC, chronic hepatitis C; EC_{50}, 50% effective concentration; GTP, guanosine triphosphate; HCV, hepatitis C virus; HPLC, high-performance liquid chromatography; IMPDH, inosine monophosphate dehydrogenase; IMP, inosine-5'-monophosphate; IRES, internal ribosome entry site; kb, kilobase; mRNA, messenger RNA; NS, nonstructural protein; nt, nucleotide; ORF, open reading frame; 4-PBA, 4-phenylbutyric acid; Peg-IFN, pegylated-interferon; PHHs, primary human hepatocytes; RACE, rapid amplification of cDNA ends; RBV, ribavirin; RL, renilla luciferase; RMP, RBV 5'-monophosphate; RT-PCR, reverse transcription-polymerase chain reaction; siRNA, small interfering RNA; miRNAs, microRNAs; SNP, single-nucleotide polymorphism; SVR, sustained virologic response; UTR, untranslated region.

From the [1]Department of Tumor Virology, Okayama University Graduate School of Medicine, Dentistry, and Pharmaceutical Sciences, Okayama, Japan; [2]School of Pharmacy, Shujitsu University, Okayama, Japan; and [3]Department of Drug Informatics, Faculty of Pharmaceutical Sciences, Okayama University, Okayama, Japan.

Received November 6, 2012; accepted March 19, 2013.

This work was supported by a grant-in-aid for research on hepatitis from the Ministry of Health, Labor and Welfare of Japan.

The main hurdle to resolving the side-effect profile is that the anti-HCV mechanism of RBV is not well understood, although several possible mechanisms have been proposed.[5,6] To date, there has been no cell-culture system enabling analysis of the anti-HCV mechanism of RBV at clinically achievable concentrations (5-14 μM), because the human hepatoma cell line, HuH-7, which has been the only cell line available for robust HCV replication, is not sensitive to RBV.[5,7,8] Indeed, we also observed that the 50% effective concentration (EC_{50}) of RBV against HCV RNA replication in our developed HuH-7-derived assay system (OR6), in which the genome-length HCV RNA (O strain of genotype 1b) encoding renilla luciferase (RL) replicates efficiently, was more than 100 μM, and 50% cytotoxic concentration (CC_{50}) was also more than 100 μM.[9,10]

On the other hand, we recently found that a new human hepatoma cell line, Li23, whose gene expression profile was distinct from that of HuH-7, enabling efficient HCV RNA replication and persistent HCV production, was sensitive to RBV.[10-12] Indeed, the EC_{50} value of RBV against HCV RNA replication in our developed Li23-derived assay system (ORL8), which is comparable to the OR6 assay system, was 8.7 μM, and the CC_{50} value was more than 100 μM.[10] It was noteworthy that this EC_{50} value was equivalent to the clinically achievable concentrations of RBV. Therefore, this finding led us to analyze the anti-HCV mechanism of RBV, and, consequently, we found that the anti-HCV activity of RBV was mediated by the inhibition of inosine monophosphate dehydrogenase (IMPDH), and that IMPDH was required for HCV RNA replication.[10]

From these findings, we anticipated that the comparative analysis of RBV-sensitive ORL8 cells and RBV-resistant OR6 cells would lead to the identification of host factor(s) determining the anti-HCV activity of RBV. Here, we report the finding that adenosine kinase (ADK) is an essential determinant of the anti-HCV activity of RBV.

Materials and Methods

Cell Cultures. HuH-7- and Li23-derived cells and PH5CH8 cells were maintained as described previously.[11] HT17 cells were cultured in Dulbecco's modified Eagle's medium supplemented with 10% fetal bovine serum. Primary human hepatocytes (PHHs; PhoenixBio, Higashihiroshima, Japan) were also maintained in the medium for the Li23-derived cells.

Reagents. RBV was kindly provided by Yamasa (Chiba, Japan).

Inosine-5'-monophosphate (IMP) and nucleoside triphosphates (cytidine triphosphate, uridine triphosphate, adenosine triphosphate, and guanosine triphosphate [GTP]) were also purchased from Yamasa. ABT-702 was purchased from Calbiochem (San Diego, CA). 5-azacytidine (5azaC) and 4-phenylbutyric acid (4-PBA) were purchased from Sigma-Aldrich (St. Louis, MO).

Western Blotting Analysis. Preparation of cell lysates, sodium dodecyl sulfate polyacrylamide gel electrophoresis, and immunoblotting analysis were performed as previously described.[13] Polyclonal-ADK (ab54818; Abcam, Cambridge, MA), monoclonal-ADK (F-5; Santa Cruz Biotechnology, Santa Cruz, CA), and β-actin (AC-15; Sigma-Aldrich) antibodies (Abs) were used.

Reverse-Transcription Polymerase Chain Reaction. Reverse-transcription polymerase chain reaction (RT-PCR) was performed to detect ADK messenger RNA (mRNA), as described previously,[14] using the primer sets (ADKF and ADKR; ADK-5'-untranslated region [UTR]-187nts and ADK-5'-UTR checkR) listed in Supporting Table 1.

Quantitative RT-PCR. Quantitative RT-PCR analysis for ADK mRNA was performed using a real-time LightCycler PCR (Roche Diagnostics, Indianapolis, IN), as described previously,[11] with the primer sets (ADKF and ADKR; ADK-5'UTR-384nts and ADK-5'UTR checkR; ADK-5'UTR-318nts and ADK-5'UTR checkR; ADK-5'UTR-187nts and ADK-5'UTR checkR; ADK-5'UTR-125nts and ADK-5'UTR checkR) listed in Supporting Table 1.

RL Assay. RL assay was performed as described previously.[9] Experiments were performed at least in triplicate.

High-Performance Liquid Chromatography Analysis. Quantitative high-performance liquid chromatography (HPLC) analysis was performed using the

Address reprint requests to: Nobuyuki Kato, Ph.D., Department of Tumor Virology, Okayama University Graduate School of Medicine, Dentistry, and Pharmaceutical Sciences, 2-5-1 Shikata-cho, Okayama 700-8558, Japan. E-mail: nkato@md.okayama-u.ac.jp; fax: (81)86-235-7392.

View this article online at wileyonlinelibrary.com.

DOI 10.1002/hep.26421

Potential conflict of interest: Nothing to report.

Additional Supporting Information may be found in the online version of this article.

extract from the OR6 or ORL8 cells treated with 50 μM of RBV for 8 hours. HPLC analysis was performed as described previously.[15]

RNA Interference. Small interfering RNA (siRNA) duplexes targeting the coding regions of human ADK (catalog no.: M-009687-01; Dharmacon, Inc., Lafayette, CO) were chemically synthesized. A nontargeting siRNA duplex (catalog no.: D-001206-13; Dharmacon) was also used as a control. ORL8 cells were transfected with the indicated siRNA duplexes using Oligofectamine (Invitrogen, Carlsbad, CA).[10]

Ectopic Expression of ADK. The methods of plasmid construction for ectopic expression of ADK and retroviral infection using the constructed plasmids are described in the Supporting Materials.

Plasmid Construction and Internal Ribosome Entry Site Activity Assay. The method of plasmid construction for internal ribosome entry site (IRES) activity assay is described in the Supporting Materials. The dual luciferase reporter assay for IRES activity was performed by the method described previously.[14]

Statistical Analysis. Data are presented as means ± standard deviation. The Student unpaired *t* test was performed for statistical analysis between the two groups, and the difference was considered significant at $P < 0.05$.

Results

High Expression Level of ADK in ORL8 Cells. To identify the host factor responsible for the difference in RBV responses between Li23-derived ORL8 and HuH-7-derived OR6 cells, we first recompared the previous data from complementary DNA (cDNA) microarrays using Li23 and HuH-7 cells. Although we assigned 17 genes that showed dramatic differences in expression between Li23 and HuH-7 cells,[12] none of these genes were considered to be involved in the response to RBV. Expression of IMPDH1 (NM_000883) and IMPDH2 (NM_000884), which were involved in the anti-HCV mechanism of RBV,[8,10] was also at a similar level between Li23 and HuH-7 cells or between cured ORL8 (ORL8c) and cured OR6 (OR6c) cells (Supporting Table 2).

We next attempted to verify the process of GTP reduction that is expected to occur after RBV is incorporated into cells. To this end, we performed a quantitative HPLC analysis using the extract from the OR6 or ORL8 cells treated with 50 μM of RBV for 8 hours, which is the working time of RBV against HCV RNA replication.[10] Amounts of IMP and GTP were calculated from the peak area obtained by HPLC

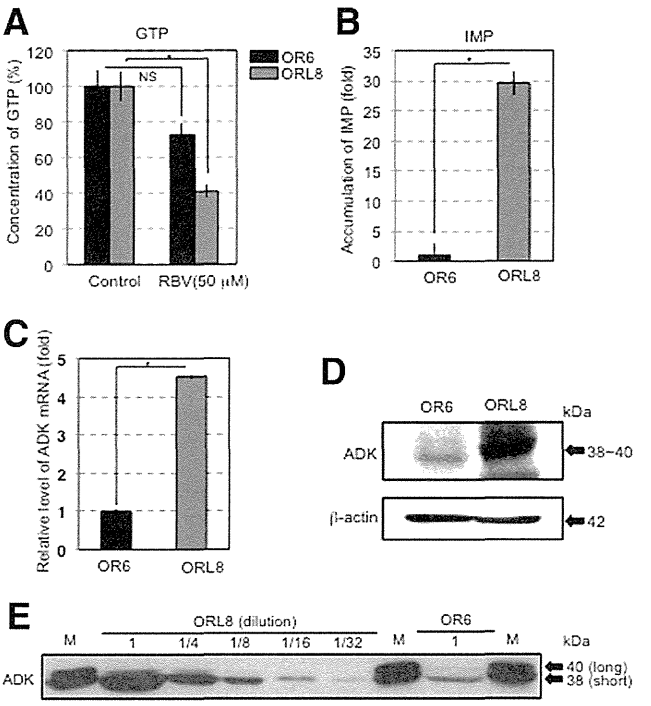

Fig. 1. Expression level of ADK in ORL8 cells was higher than that in OR6 cells. (A) Signal of GTP obtained by HPLC analysis using nts extracted from RBV-treated cells was quantified. (B) Signal of IMP obtained by HPLC analysis using nts extracted from RBV-treated cells was quantified. (C) Expression level of ADK mRNA in ORL8 cells was compared with that in OR6 cells by quantitative RT-PCR analysis. (D) Level of ADK in ORL8 cells was compared with that in OR6 cells by western blotting analysis. (E) ORL8 cell extract was diluted and then western blotting analysis was performed for the detection of ADK. Two isoforms of ADK (40 and 38 kDa) were loaded as molecular markers. Experiments (A-C) were performed in triplicate. $^*P < 0.05$; NS, not significant.

analysis. Volume of cells was calculated from the mean diameter of cells, and we found 10^6 cells to be equivalent to 1.1 mm^3. We assumed that the extracted nucleotides (nts) were uniformly distributed in the cell aqueous volume. As expected, the level of intracellular GTP in ORL8 cells showed a significant (60%) reduction, whereas that in OR6 cells showed only a 27% reduction (Fig. 1A and Supporting Fig. 1A-D). These results support our previous finding that the inhibitory effect of RBV on HCV RNA replication in ORL8 cells is stronger than that in OR6 cells.[10]

In addition, we noticed an unexpected phenomenon: A substantial accumulation of IMP occurred as the result of IMPDH inhibition in ORL8 cells, but not in OR6 cells. The IMP level in ORL8 cells became approximately 30 times higher than that in OR6 cells (Fig. 1B and Supporting Fig. 1A-D). However, no additive effect of inosine (up to 100 μM) on HCV RNA replication in ORL8 cells was observed (Supporting Fig. 2).

It has been reported that RBV is metabolized *in vivo* through RBV 5'-monophosphate (RMP), a

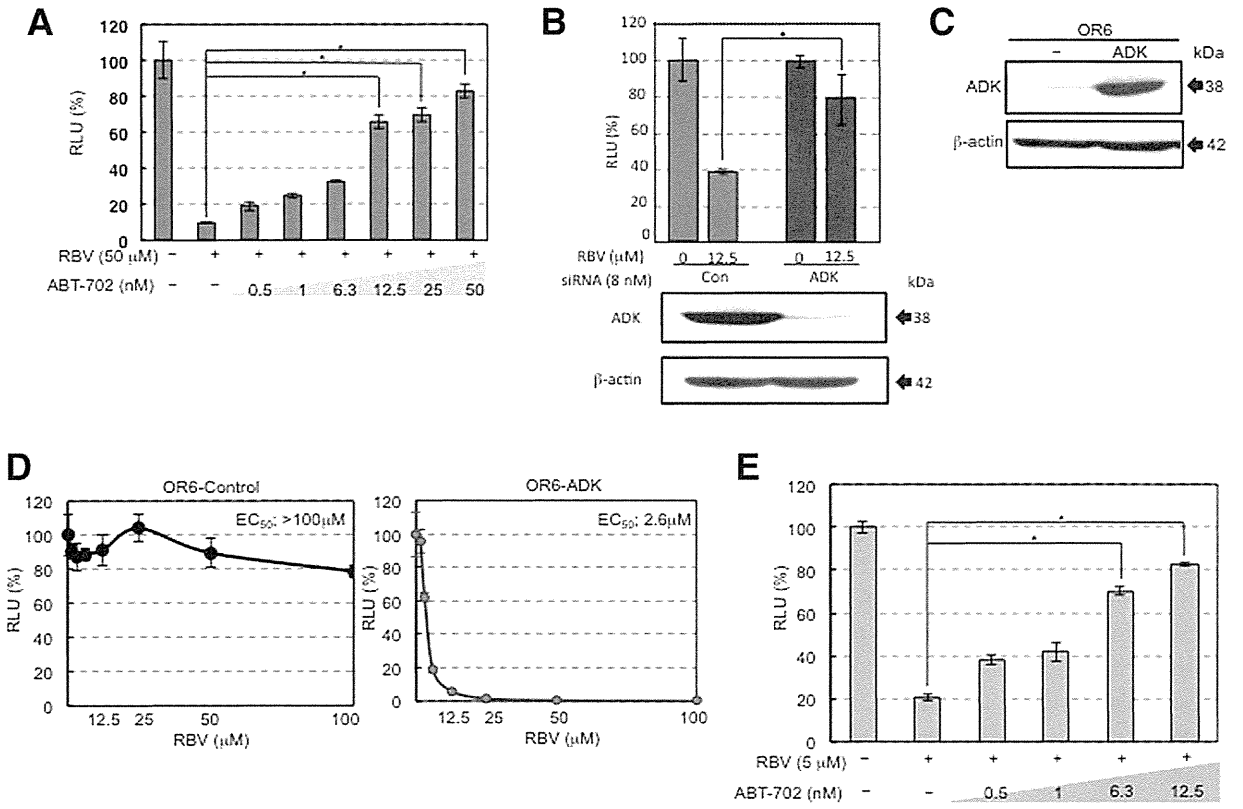

Fig. 2. ADK is a determining host factor for the anti-HCV activity of RBV. (A) ORL8 cells were cotreated with RBV (50 μM) and ABT-702 (nM) for 72 hours, after which an RL assay was performed. Relative luciferase activity (RLU) (%) calculated at each time point, when the level of luciferase activity in nontreated cells was assigned to be 100%, is shown. (B) ORL8 cells were transfected with 8 nM of siRNA targeting ADK. After 72 hours, expression levels of ADK were monitored by western blotting analysis (lower panel). ADK-knockdown ORL8 cells were treated with 12.5 μM of RBV for 72 hours, after which an RL assay was performed, as described in (A, upper panel). (C) Expression level of ADK in OR6-ADK cells was monitored by western blotting analysis. (D) OR6-ADK cells were treated with RBV for 72 hours and then an RL assay was performed as described in (A). (E) OR6-ADK cells were cotreated with RBV (5 μM) and ABT-702 (nM) for 72 hours and then an RL assay was performed, as described in (A). Experiments (A, B, D, and E) were performed in triplicate. $*P < 0.05$.

competitive inhibitor of IMPDH, by ADK.[16] Based on our findings, we expected that ADK activity might be able to control the anti-HCV activity of RBV. Indeed, microarray analysis revealed that the actual expression levels of ADK were 764 and 2,840 in OR6c and ORL8c cells, respectively. Quantitative RT-PCR analysis also showed that the mRNA level of ADK in ORL8 cells was 4.5 times higher than that in OR6 cells (Fig. 1C). Furthermore, we found that the protein level of ADK in ORL8 cells was much higher than that in OR6 cells (Fig. 1D).

On the other hand, it is known that ADK has two major isoforms: ADK-long (NM_006721) localized in the nucleus and ADK-short (NM_001123) localized in the cytoplasm.[17] ADK-long differs in the 5' UTR and initiates translation at an alternative start codon, compared to ADK-short. ADK-long is 17 amino acids longer than ADK-short. We prepared ORL8 cells stably overexpressing ORL8-derived ADK-long or ADK-short using a retroviral gene transfer system and examined its mobility in western blotting analysis. Fortunately, two isoforms were discriminable as 40 (ADK-long) and 38 kDa (ADK-short) (Fig. 1E). Using these isoforms as molecular markers, we performed semiquantitative western blotting analysis by the sample dilution method. The results revealed that the expression level of ADK-short in ORL8 cells was approximately 16 times higher than that in OR6 cells, and that ADK-long was little expressed in both cells (Fig. 1E). From these results, we assumed that the differences in ADK expression were involved in the dramatic differences in RBV sensitivity between the two cell lines. To address this assumption, we focused on the ADK-short in the following study; hereafter, ADK-short is designated as ADK.

ADK Is a Host Factor Determining the Anti-HCV Activity of RBV. To evaluate the hypothesis that ADK controls the anti-HCV activity of RBV, we first examined the effect of ABT-702, an ADK inhibitor, on the anti-HCV activity of RBV. The results revealed that ABT-702 cancelled the activity of RBV in ORL8

cells in a dose-dependent manner (Fig. 2A). Furthermore, we demonstrated that the activity of RBV was cancelled in ADK-knockdown ORL8 cells (Fig. 2B). These results suggest that the inhibition of ADK in ORL8 cells converts them from an RBV-sensitive phenotype to an RBV-resistant phenotype.

To directly demonstrate the involvement of ADK, we first prepared OR6 cells stably expressing ADK (OR6-ADK) (Fig. 2C). We were able to demonstrate that the OR6-ADK cells were dramatically converted from an RBV-resistant phenotype with an EC_{50} value of more than 100 μM to an RBV-sensitive phenotype with an EC_{50} value of 2.6 μM (Fig. 2D). We next examined whether or not the GTP reduction or IMP accumulation observed in ORL8 cells treated with RBV (Fig. 1A,B) occurs in OR6-ADK cells. The results revealed that the GTP reduction and IMP accumulation in RBV-treated OR6-ADK cells were more pronounced than in RBV-treated ORL8 cells (Supporting Fig. 3A,B). Because OR6 is a clonal cell line harboring genome-length HCV RNA, we used a polyclonal cell line (sOR) harboring HCV replicon RNA[9] to prepare sOR-ADK cells stably expressing ADK (Supporting Fig. 3C) and examined their sensitivity to RBV. sOR-ADK cells were also dramatically converted from an RBV-resistant phenotype with an EC_{50} value of more than 100 μM to an RBV-sensitive phenotype with an EC_{50} value of 6.0 μM (Supporting Fig. 3D). In addition, ORL8-ADK cells stably overexpressing ADK also showed EC_{50} values ranging from 13.2 to 1.2 μM (Supporting Fig. 3E). Furthermore, we demonstrated that the anti-HCV activity detected in OR6-ADK cells was also cancelled by ABT-702 treatment in a dose-dependent manner (Fig. 2E). Considering these results together, we conclude that ADK is a key determinant for the anti-HCV activity of RBV.

The Suppression of ADK Expression in OR6 Cells Was Not the Result of Genetic Variations or Epigenetic Alterations in the ADK Gene Promoter. To clarify the mechanism underlying the difference in ADK expression between OR6 and ORL8 cells, we first examined the nt sequences of up to several kb upstream from the transcription start point estimated from NM_001123 (31-OCT-2010) using the data of AL731576. Several possible transcription elements, such as the GC box (−12 and −187 of ADK gene), p53 response element (−252 and −585), and heat shock element (−559, −971, −1486, and −1797) were detected in up to approximately 2 kb upstream from the estimated transcription start point, but not in more 2 kb. Accordingly, we amplified approximately 2 kb including the 5' UTR (187 nts estimated by NM_001123 [31-OCT-2010]) by PCR using DNA prepared from ORL8 or OR6 cells, and each PCR product was inserted into pGL4.10-luc2 for the sequence analysis and reporter analysis of gene promoter activity. Sequence analysis confirmed that the sequences of the inserts were the same as the sequence data of the ADK gene (AL731576), except in the case of a single-nucleotide polymorphism (SNP) [rs10824095; C for ORL8 cells and T for OR6 cells] located 20 bases upstream from the initiation codon. Luciferase reporter assay using ORL8c cells revealed that the promoter activity of OR6 origin was almost equal to that of ORL8 origin (Supporting Fig. 4A), indicating that the detected SNP was not involved in the level of promoter activity.

We next evaluated the epigenetic effects on ADK expression level. The results revealed that the expression level of ADK mRNA in OR6 cells was not enhanced in the cells treated with 5azaC and/or 4-PBA for 48 hours (Supporting Fig. 4B). Moreover, the protein level of ADK was not increased in the OR6 cells treated with 5azaC for 6 days (Supporting Fig. 4C). Taken together, these results suggest that the low level of ADK mRNA in OR6 cells was not the result of genetic polymorphisms or epigenetic alternations in the ADK gene promoter region.

The Differential ADK Expression Between OR6 and ORL8 Cells Was Not Mediated by a microRNA Control Mechanism. To explain the above-described gap between the 4.5-fold difference in the mRNA level and the 16-fold difference in the protein level (Fig. 1C,E), we hypothesized that the 3' UTR of ADK mRNA was different in the length or nt sequences between OR6 and ORL8 cells, and that such differences affected the control mechanism by microRNA (miRNA). To test this hypothesis, we first performed 3' rapid amplification of cDNA ends (RACE) analysis on ADK mRNA using total RNA prepared from OR6 or ORL8 cells. Sequence analysis using more than 45 cDNA clones obtained from each cell line was carried out. 3' UTRs of four different lengths were detected in both OR6 and ORL8 cells, because four potential poly(A) additional signals were present in the downstream ADK open reading frame (ORF) (Supporting Fig. 5). The results revealed no qualitative difference of 3' UTR species between OR6 and ORL8 cells (Supporting Fig. 5).

Because the 3' UTR of ADK mRNA contained the seed sequences of miR-182, miR-203, mir-125a-3p, and miR-106b (Supporting Fig. 5), we assumed that

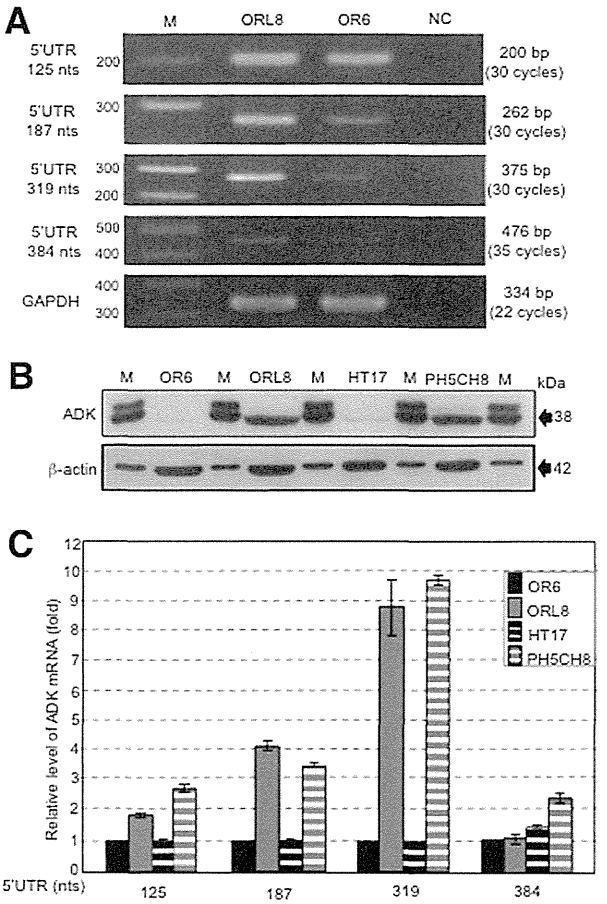

Fig. 3. Level of ADK mRNA possessing long 5' UTR was correlated with the expression level of ADK. (A) Total RNAs prepared from ORL8 and OR6 cells were subjected to RT-PCR using the primer sets (Supporting Table 1) for various lengths of 5' UTR of ADK mRNA. (B) Expression levels of ADK were compared by western blotting analysis. The two molecular markers of ADK shown in Fig. 1E were loaded on every two lanes. (C) Amounts of 5' UTR species of ADK mRNAs were compared by quantitative RT-PCR analysis using the primer sets described in (A). Experiments were performed in triplicate.

the difference in expression levels of these miRNAs causes the different protein levels of ADK. To examine this possibility, we performed an miRNA microarray analysis between OR6 and ORL8 cells. This analysis revealed very low expression levels (measured values of less than 7) of miR-182, miR203, and miR-125a-3p in both cell lines. Although only miR-106b was moderately expressed (measured value of approximately 300) in OR6 and ORL8 cells, the values obtained from both cell lines were almost the same. From these results, these miRNAs may not participate in the translational regulation of ADK mRNAs in OR6 and ORL8 cells.

The 5' UTR of ADK mRNA in ORL8 Cells Was Longer Than That in OR6 Cells. To explain the dramatic difference in ADK expression between ORL8 and OR6 cells, we next focused on the 5' UTR. To date, two different lengths of 5' UTR (384 nts in accession number NM_001123[25-MAR-2011] and 187 nts in accession numbers NM_001123[31-OCT-2010] and HSU_50196) have been deposited in GeneBank. Because the 384 nts form has been considered to be a unique species in testis tissue, we performed 5' RACE analysis to determine the length of the 5' UTR of ADK mRNA in ORL8 or OR6 cells. Sequence analysis was carried out using more than 20 cDNA clones obtained from each cell line. Consequently, we obtained 319 and 125 nts as the major 5' UTR species in ORL8 and OR6 cells, respectively. We confirmed these results by RT-PCR analysis using four different primer sets for the 5' UTR (Fig. 3A). The amount of 384 nts species in ORL8 cells was estimated to be less than one thirtieth the amount of the 319-nts species (Fig. 3A). These results indicate that the length of 5' UTR in ORL8 cells is longer than that in OR6 cells.

From these results, we considered the possibility that the length of the 5' UTR is associated with the protein level of ADK. To test this possibility, we first compared the expression levels of ADK in various human hepatoma cell lines and human immortalized hepatocyte lines. Low expression level of ADK was observed in HT17 and Hep3B cells as well as OR6 cells, although the other cell lines, including ORL8, HuH-6, HepG2, HLE, and PH5CH8 cells, showed high expression level of ADK (Fig. 3B and Supporting Fig. 6). We next performed quantitative RT-PCR analysis on the 5' UTR using total RNAs from OR6, ORL8, HT17, and PH5CH8 cells. Consequently, we found that the 319 nts species of the 5' UTR was abundant in PH5CH8 cells, but not in HT17 cells (Fig. 3C), indicating good correlation between the amount of 319 nts species and the amount of ADK protein (Fig. 3B,C). These results suggest that the 319 nts species of 5' UTR is involved in the high protein level of ADK.

The Long-Form 5' UTR of ADK mRNA Possessed IRES Activity. From the results of 5' UTR analysis, we assumed that the 319 nts species of the 5' UTR possesses IRES activity because it is GC rich (72%) and highly structured (estimated $\Delta G = -110.7$ kcal/mol), and because it contains an upstream ORF for 70 amino acids. To test this assumption, we used a bicistronic dual luciferase reporter assay system for the detection of IRES activity (Fig. 4A). As a positive control, we constructed a pGL4-based reporter plasmid containing HCV IRES (377 nts; 341 nts in the 5' UTR plus the first 36 nts in the Core-encoding

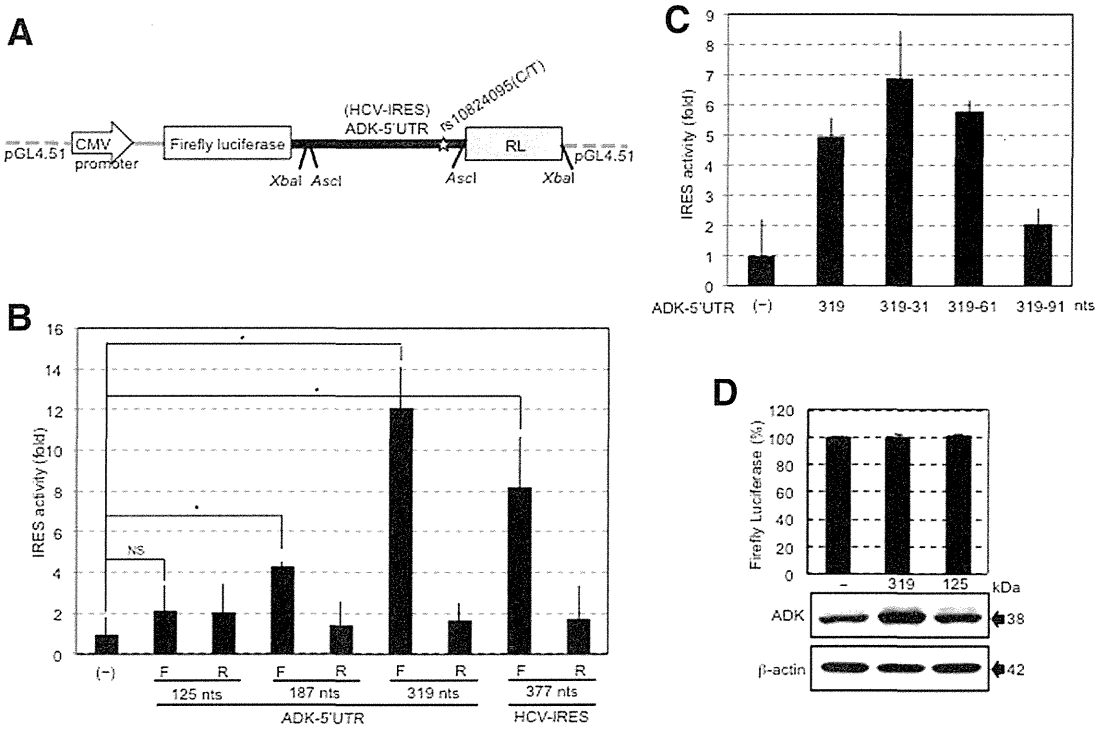

Fig. 4. Long-form 5' UTR of ADK mRNA possessed IRES activity. (A) Partial structure of the plasmid used as a dicistronic dual reporter assay system. (B) ORL8c cells were transfected with the plasmid as shown in (A). After 48 hours, a dual luciferase assay was performed. The ratio of the RL activity to firefly luciferase activity was calculated. The relative value calculated at each sample, when the ratio in the control vector-transfected cells (−) was assigned to be 1, is presented. F and R indicate the forward and reverse direction of insert in the reporter plasmid, respectively. (C) Deletion mutant analysis of the 5' UTR in IRES assay. IRES assay was performed using ORL8c cells transfected with the reporter plasmid containing the deleted forms of the 5' UTR, as described in (B). (D) ADK expression derived from the long-form 5' UTR transcript was more productive than that from the short-form 5' UTR transcript. OR6c cells were transfected with the plasmid, in which the *XbaI* fragment of the plasmid used for HCV IRES activity assay was replaced by the ADK ORF possessing the 5' UTR of 319 or 125 nts. After 48 hours, western blotting analysis was performed. Firefly luciferase activities were measured to check equal transfection efficiency. Experiments (B and C) were performed in triplicate. $*P < 0.05$; NS, not significant.

region). We next replaced the HCV IRES structure in this plasmid with several different lengths (forward or reverse direction) of the 5' UTR derived from ORL8 cells. ORL8c cells were transfected with these plasmids, and at 48 hours after transfection, dual luciferase assays were performed. Consequently, we found that the forward 319 nts, but not the forward 125 nts, of 5' UTR clearly showed IRES activity at the same level as HCV IRES (Fig. 4B). The 187 nts species also showed weak IRES activity (Fig. 4B). None of the 5' UTR species with reverse direction and none of the HCV IRES with reverse direction showed any IRES activities (Fig. 4B). Furthermore, similar results were obtained in the genome-length HCV RNA-replicating OL8 cells and their cured cells (OL8c) (Supporting Fig. 7A,B), suggesting that IRES activity does not depend on cell strains or HCV RNA replication. In addition, we did not observe any effects of an SNP (rs10824095), which was located 20 bases upstream from the initiation codon, on the IRES activities of OR6 and ORL8 cell-derived 5' UTRs (319 nts) (Supporting Fig. 8).

To identify the entry site of the 40S ribosome in the IRES region, we prepared three deletion mutants (deleted upstream 30, 60, and 90 nts from the initiation codon) of the 5' UTR and measured their IRES activities in ORL8c cells. The results revealed that the deletion up to 60 nts from the initiation codon did not decrease IRES activity, but the 90 nts deletion abolished IRES activity (Fig. 4C). Similar results were also obtained in OL8 and OL8c cells (Supporting Fig. 7C,D). These results suggest that the entry site of the 40S ribosome is between 60 and 90 nts upstream from the initiation codon, and that the region from 319 to 61 nts upstream from the initiation codon is necessary for the IRES activity. It is noteworthy that this region forms a stable secondary structure (estimated $\Delta G = -108.4$ kcal/mol) (Supporting Fig. 7E). Furthermore, we demonstrated that ADK expression derived from the long-form 5' UTR transcript was

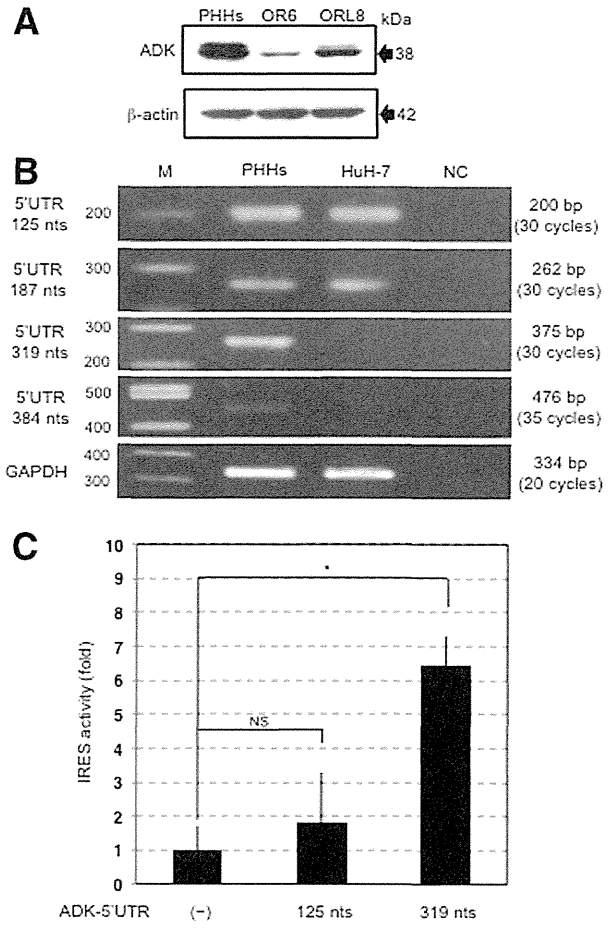

Fig. 5. Long-form 5' UTR of ADK mRNA functioned as an IRES in PHHs. (A) ADK expression level in PHHs was compared with those in OR6 and ORL8 cells by western blotting analysis. (B) Total RNAs prepared from PHHs and HuH-7 cells were subjected to RT-PCR analysis using the primer sets described in Fig. 3A. (C) PHHs were transfected with the plasmid shown in Fig. 4A. After 48 hours, a dual luciferase assay was performed as described in Fig. 4B. Experiments (B and C) were performed in triplicate. $*P < 0.05$; NS, not significant.

more productive than the expression from the short-form 5' UTR transcript in OR6c cells (Fig. 4D).

The Long-Form 5' UTR of ADK mRNA Functioned as an IRES in Primary Human Hepatocytes. To obtain a final conclusion, we examined whether the novel mechanism in ADK translation plays a role in PHHs. We first examined ADK expression level in PHHs, and the results revealed that ADK protein level was higher in PHHs than in ORL8 cells (Fig. 5A). We next performed RT-PCR analysis using the primer sets used in Fig. 3A to examine the amounts of 319 and 125 nts forms of the 5' UTR. The results showed that the 319 nts species was the major 5' UTR species in PHHs, but not in HuH-7 cells, which are the parent of OR6 cells (Fig. 5B), indicating a good correlation between the amount of 319 nts species and the amount of ADK protein in PHHs. Finally, we demonstrated that the 319 nts form, but not the 125 nts form, of 5' UTR clearly showed IRES activity in PHHs (Fig. 5C).

Considering all these results together, we conclude that not only ORL8 cells, but also PHHs express the long-form 5' UTR of ADK mRNA possessing IRES activity and then produce high levels of ADK, which works as an RBV kinase.

Discussion

In this study, we identified, for the first time, a host factor ADK whose expression level could control the anti-HCV activity of RBV. Furthermore, we found that the expression level of ADK was associated with the amount of ADK mRNA possessing long 5' UTR exhibiting IRES activity. This finding suggests that the RBV sensitivity on HCV RNA replication is regulated by the IRES-dependent translation of ADK mRNA. If ADK expression levels or activity differ between patients with CHC, it may be a useful therapeutic target.

It has recently been reported that a functional SNP (rs1127354; major C and minor A) in inosine triphosphatase was the most significant SNP associated with RBV-induced anemia.[18] In this context, we hypothesized that this SNP is associated with the expression level of ADK. To test this hypothesis, we examined the status of rs1127354 in ORL8 and PH5CH8 cells showing high expression levels of ADK and in OR6 and Hep3B cells showing low expression levels of ADK. The results revealed that all cell lines showed the major C of the SNP, suggesting that rs1127354 is not associated with the expression level of ADK.

The most striking highlight in this study is the IRES activity found in ADK mRNA. It has recently been reported that cellular IRES-mediated translation is activated by many physiological and pathological stress conditions in eukaryotic cells.[19] To achieve efficient IRES-dependent translation, some triggers will be needed. However, HCV RNA replication was not such a trigger, in the present study, because a similar level of IRES activity was observed in both OL8c cured cells and genome-length HCV RNA-replicating OL8 cells (Supporting Fig. 7A-D). The addition of adenosine did not act as a trigger for IRES (Supporting Fig. 9). Another possible explanation for the high level of ADK in ORL8 cells would be the involvement of one or more miRNA(s) in stabilizing the IRES-containing ADK mRNA, as reported in HCV RNA.[20] To test this possibility, we performed comparative miRNA microarray analysis using ORL8, PH5CH8, OR6, and HT17 cells. The results revealed that nts 1-8 of miR-

424, whose expression levels in ORL8 and PH5CH8 cells were several times higher than those in OR6 and HT17 cells, showed base pairs in the nt 61-68 upstream initiation codon of ADK mRNA. It was noticed that this region in ADK mRNA overlaps the region (nt 60-90 upstream initiation codon of ADK mRNA) identified as the entry site of the 40S ribosome. However, a preliminary experiment showed that overexpression of miR-424 in ORL8 or OR6 cells did not enhance the translation of ADK (Supporting Fig. 10), suggesting that miR-424 is not associated with the high level of ADK in ORL8 cells. The possibility remains that other miRNA(s) participate in the up-regulation of ADK.

At this time, we have identified ADK as a host factor that controls the anti-HCV activity of RBV and clarified the molecular mechanism underlying regulation with ADK. Furthermore, we demonstrated that such a novel mechanism plays a role in PHHs. From our finding, we suggest that ADK expression is artfully regulated both at the transcription and translation stage. Although we identified ADK, which participates in nucleotidic metabolism, as an enzyme functionally controlled by the specific expression of an IRES-containing mRNA, there may be other gene products controlled by a similar mechanism.

Acknowledgments: The authors thank Naoko Kawahara, Takashi Nakamura, and Keiko Takeshita for their technical assistance.

References

1. Lindenbach BD, Rice CM. Unravelling hepatitis C virus replication from genome to function. Nature 2005;436:933-893.
2. Ghany MG, Nelson DR, Strader DB, Thomas DL, Seeff LB. An update on treatment of genotype 1 chronic hepatitis C virus infection: 2011 practice guideline by the American Association for the Study of Liver Diseases. HEPATOLOGY 2011;54:1433-1444.
3. Jacobson IM, McHutchison JG, Dusheiko G, Di Bisceglie AM, Reddy KR, Bzowej NH, et al. Telaprevir for previously untreated chronic hepatitis C virus infection. N Engl J Med 2011;364:2405-2416.
4. Poordad F, McCone J, Jr., Bacon BR Bruno S, Manns MP, Sulkowski MS, et al. Boceprevir for untreated chronic HCV genotype 1 infection. N Engl J Med 2011;364:1195-1206.
5. Feld JJ, Hoofnagle JH. Mechanism of action of interferon and ribavirin in treatment of hepatitis C. Nature 2005;436:967-972.
6. Paeshuyse J, Dallmeier K, Neyts J. Ribavirin for the treatment of chronic hepatitis C virus infection: a review of the proposed mechanisms of action. Curr Opin Virol 2011;1:590-598.
7. Thomas E, Feld JJ, Li Q, Hu Z, Fried MW, Liang TJ. Ribavirin potentiates interferon action by augmenting interferon-stimulated gene induction in hepatitis C virus cell culture models. HEPATOLOGY 2011;53:32-41.
8. Zhou S, Liu R, Baroudy BM, Malcolm BA, Reyes GR. The effect of ribavirin and IMPDH inhibitors on hepatitis C virus subgenomic replicon RNA. Virology 2003;310:333-342.
9. Ikeda M, Abe K, Dansako H, Nakamura T, Naka K, Kato N. Efficient replication of a full-length hepatitis C virus genome, strain O, in cell culture, and development of a luciferase reporter system. Biochem Biophys Res Commun 2005;329:1350-1359.
10. Mori K, Ikeda M, Ariumi Y, Dansako H, Wakita T, Kato N. Mechanism of action of ribavirin in a novel hepatitis C virus replication cell system. Virus Res 2011;157:61-70.
11. Kato N, Mori K, Abe K, Dansako H, Kuroki M, Ariumi Y, et al. Efficient replication systems for hepatitis C virus using a new human hepatoma cell line. Virus Res 2009;146:41-50.
12. Mori K, Ikeda M, Ariumi Y, Kato N. Gene expression profile of Li23, a new human hepatoma cell line that enables robust hepatitis C virus replication: comparison with HuH-7 and other hepatic cell lines. Hepatol Res 2010;40:1248-1253.
13. Kato N, Sugiyama K, Namba K, Dansako H, Nakamura T, Takami M, et al. Establishment of a hepatitis C virus subgenomic replicon derived from human hepatocytes infected in vitro. Biochem Biophys Res Commun 2003;306:756-766.
14. Dansako H, Naganuma A, Nakamura T, Ikeda F, Nozaki A, Kato N. Differential activation of interferon-inducible genes by hepatitis C virus core protein mediated by interferon stimulated response element. Virus Res 2003;97:17-30.
15. Takatori S, Kanda H, Takenaka K, Wataya Y, Matsuda A, Fukushima M, et al. Antitumor mechanisms and metabolism of the novel antitumor nucleoside analogues, 1-(3-C-ethynyl-beta-D-ribo-pentofuranosyl)-cytosine and 1-(3-C-ethynyl-beta-D-ribo-pentofuranosyl)uracil. Cancer Chemother Pharmacol 1999;44:97-104.
16. Streeter DG, Witkowski JT, Khare GP, Sidwell RW, Bauer RJ, Robins RK, Simon LN. Mechanism of action of 1-β-D-ribofuranosyl-1,2,4-triazole-3-carboxamide (Virazole), a new broad-spectrum antiviral agent. Proc Natl Acad Sci U S A 1973;70:1174-1178.
17. Cui XA, Singh B, Park J, Gupta RS. Subcellular localization of adenosine kinase in mammalian cells: the long isoform of AdK is localized in the nucleus. Biochem Biophys Res Commun 2009;388:46-50.
18. Fellay J, Thompson AJ, Ge D, Gumbs CE, Urban TJ, Shianna KV, et al. ITPA gene variants protect against anaemia in patients treated for chronic hepatitis C. Nature 2010;464:405-408.
19. Komar AA, Hatzoglou M. Cellular IRES-mediated translation: the war of ITAFs in pathophysiological states. Cell Cycle 2011;10:229-240.
20. Shimakami T, Yamane D, Jangra RK, Kempf BJ, Spaniel C, Barton DJ, Lemon SM. Stabilization of hepatitis C virus RNA by an Ago2-miR-122 complex. Proc Natl Acad Sci U S A 2012;109:941-946.

OPEN ACCESS Freely available online

PLOS ONE

New Preclinical Antimalarial Drugs Potently Inhibit Hepatitis C Virus Genotype 1b RNA Replication

Youki Ueda[1], Midori Takeda[1], Kyoko Mori[1], Hiromichi Dansako[1], Takaji Wakita[2], Hye-Sook Kim[3], Akira Sato[3], Yusuke Wataya[3], Masanori Ikeda[1], Nobuyuki Kato[1]*

1 Department of Tumor Virology, Okayama University Graduate School of Medicine, Dentistry, and Pharmaceutical Sciences, Shikata-cho, Okayama, Japan, **2** Department of Virology II, National Institute of Infectious Disease, Toyama, Shinjuku-ku, Tokyo, Japan, **3** Department of Drug Informatics, Faculty of Pharmaceutical Sciences, Okayama University, Tsushima-naka, Okayama, Japan

Abstract

Background: Persistent hepatitis C virus (HCV) infection causes chronic liver diseases and is a global health problem. Although new triple therapy (pegylated-interferon, ribavirin, and telaprevir/boceprevir) has recently been started and is expected to achieve a sustained virologic response of more than 70% in HCV genotype 1 patients, there are several problems to be resolved, including skin rash/ageusia and advanced anemia. Thus a new type of anti-HCV drug is still needed.

Methodology/Principal Findings: Recently developed HCV drug assay systems using HCV-RNA-replicating cells (e.g., HuH-7-derived OR6 and Li23-derived ORL8) were used to evaluate the anti-HCV activity of drug candidates. During the course of the evaluation of anti-HCV candidates, we unexpectedly found that two preclinical antimalarial drugs (N-89 and its derivative N-251) showed potent anti-HCV activities at tens of nanomolar concentrations irrespective of the cell lines and HCV strains of genotype 1b. We confirmed that replication of authentic HCV-RNA was inhibited by these drugs. Interestingly, however, this anti-HCV activity did not work for JFH-1 strain of genotype 2a. We demonstrated that HCV-RNA-replicating cells were cured by treatment with only N-89. A comparative time course assay using N-89 and interferon-α demonstrated that N-89-treated ORL8 cells had more rapid anti-HCV kinetics than did interferon-α-treated cells. This anti-HCV activity was largely canceled by vitamin E. In combination with interferon-α and/or ribavirin, N-89 or N-251 exhibited a synergistic inhibitory effect.

Conclusions/Significance: We found that the preclinical antimalarial drugs N-89 and N-251 exhibited very fast and potent anti-HCV activities using cell-based HCV-RNA-replication assay systems. N-89 and N-251 may be useful as a new type of anti-HCV reagents when used singly or in combination with interferon and/or ribavirin.

Citation: Ueda Y, Takeda M, Mori K, Dansako H, Wakita T, et al. (2013) New Preclinical Antimalarial Drugs Potently Inhibit Hepatitis C Virus Genotype 1b RNA Replication. PLoS ONE 8(8): e72519. doi:10.1371/journal.pone.0072519

Editor: Hak Hotta, Kobe University, Japan

Received April 11, 2013; **Accepted** July 5, 2013; **Published** August 30, 2013

Funding: This study was supported by a grant-in-aid for research on hepatitis from the Ministry of Health, Labor and Welfare of Japan. The funders had no role in study design, data collection and analysis, decision to publish, or preparation of the manuscript.

Competing Interests: The authors have declared that no competing interests exist.

* E-mail: nkato@md.okayama-u.ac.jp

Introduction

Hepatitis C virus (HCV) infection causes chronic hepatitis, which can lead to liver cirrhosis and hepatocellular carcinoma. Approximately 170 million people are infected with HCV worldwide, making HCV infection a serious global health problem [1]. HCV is an enveloped virus with a positive single-stranded RNA genome, and belongs to the *Flaviviridae* family. The HCV genome encodes a large polyprotein precursor of approximately 3000 amino acids, which is cleaved into 10 proteins in the following order: Core, envelope 1 (E1), E2, p7, non-structural 2 (NS2), NS3, NS4A, NS4B, NS5A, and NS5B [2,3].

Until last year, the combination of pegylated-interferon (PEG-IFN) with ribavirin (RBV) was the standard therapy, resulting in a sustained virologic response (SVR) in about half of the patients receiving this treatment [4]. Two inhibitors of HCV NS3-4A protease, telaprevir and boceprevir, were recently approved as the first directly acting antiviral reagents for the treatment of HCV genotype 1, and have been used in combination with PEG-IFN and RBV [5]. The SVR rate in the treatment of HCV genotype 1 using the new triple therapy is expected to be more than 70% [6,7]. However, several severe side effects have appeared, such as skin rash by telaprevir, ageusia by boceprevir, and advanced anemia by telaprevir/boceprevir [6,7]. Furthermore, the rapid emergence of resistant viruses by treatment with telaprevir or boceprevir is also a serious problem [8,9], since it is expected that these resistant viruses will exhibit a resistant phenotype against other NS3-4A inhibitors developed in the future [10]. Therefore, a new type of anti-HCV reagent without severe side effects or emergence of resistant virus is still needed [10], although several anti-HCV candidates, such as NS5A and NS5B inhibitors, are currently in phase II–III development [11].

To date, human hepatoma cell line HuH-7-derived cells are used as the only the preferred culture system for robust HCV replication, and most studies on anti-HCV reagents are currently

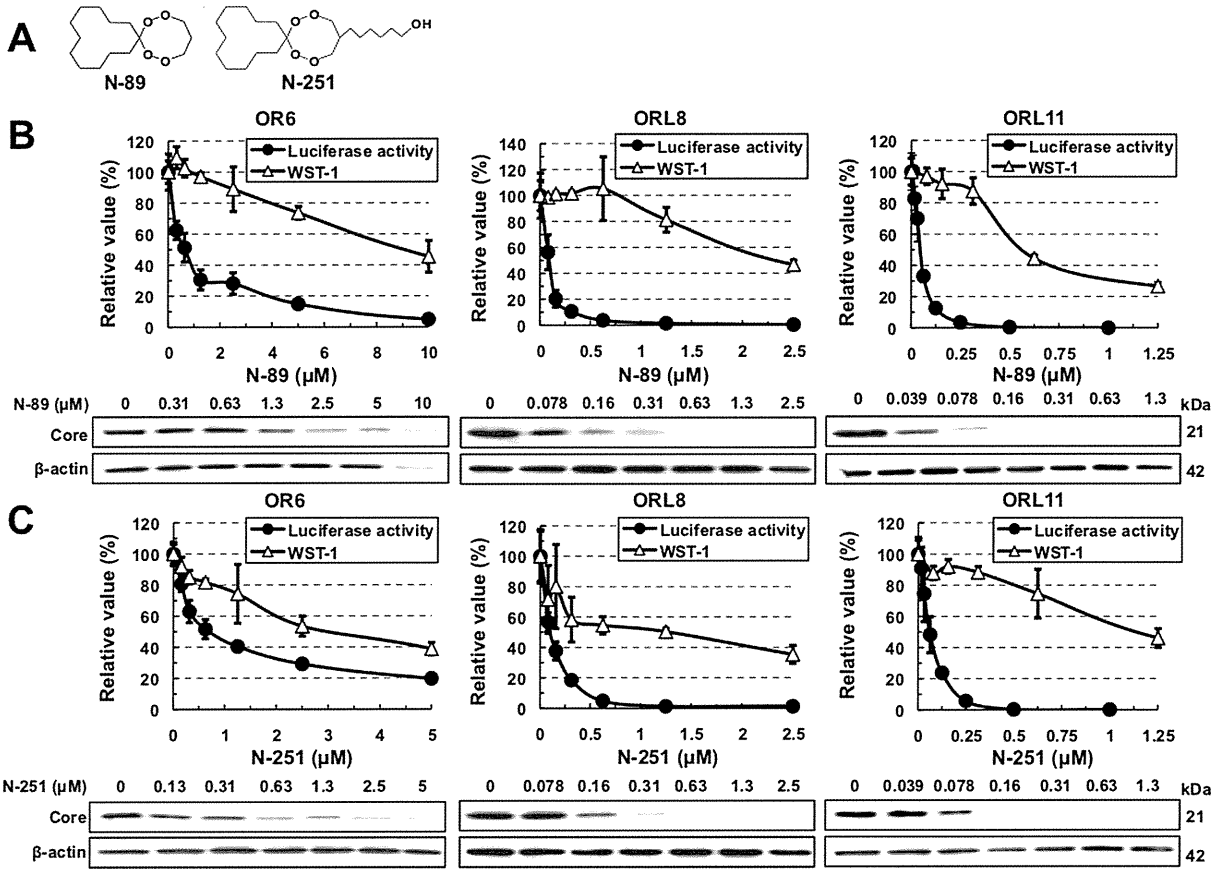

Figure 1. Anti-HCV activities of N-89 and N-251 detected in the OR6, ORL8, and ORL11 assays. (A) Structures of N-89 and N-251. (B) Effects of N-89 on genome-length HCV-RNA replication. OR6, ORL8, and ORL11 cells were treated with N-89 for 72 hrs, followed by RL assay (black circles in the upper panel) and WST-1 assay (open triangles in the upper panel). The relative value (%) calculated at each point, when the level in non-treated cells was assigned as 100%, is presented here. Data are expressed as the means±standard deviation of triplicate assays. Western blot analysis of the treated cells for the HCV Core was also performed (lower panel). β-actin was used as a control for the amount of protein loaded per lane. (C) Effects of N-251 on genome-length HCV-RNA replication. The RL assay, WST-1 assay, and Western blot analysis were performed as described in (B).
doi:10.1371/journal.pone.0072519.g001

carried out using an HuH-7-derived cell culture system [12]. We also developed an HuH-7-derived drug assay system (OR6), in which genome-length HCV-RNA (O strain of genotype 1b derived from an HCV-positive healthy carrier) encoding renilla luciferase (RL) efficiently replicates [13]. Such reporter assay systems could save time and facilitate the mass screening of anti-HCV reagents, since the values of luciferase correlated well with the level of HCV RNA after treatment with anti-HCV reagents [13]. Furthermore, OR6 assay system became more useful as a drug assay system [14] than the HCV subgenomic replicon-based reporter assay systems developed to date [12,15], because the older systems lack the core-NS2 regions containing structural proteins likely to be involved in the events that take place in the HCV-infected human liver. Indeed, by the screening of preexisting drugs using the OR6 assay system, we have identified mizoribine [16], statins [17], hydroxyurea [18], and teprenone [19] as new anti-HCV drug candidates, indicating that the OR6 assay system is useful for the discovery of anti-HCV reagents.

On the other hand, we recently found a new human hepatoma cell line, Li23, that enables efficient HCV-RNA replication and persistent HCV production, and we developed Li23-derived assay systems (ORL8 and ORL11) [20] that are comparable to the OR6 assay system [13]. Since we indicated that the gene expression profile of Li23 cells was distinct from that of HuH-7 cells [21], we expected that anti-HCV targets in Li23-derived cells might be distinct from those in HuH-7-derived cells. Indeed, we recently found that 10 μM (a clinically achievable concentration) of RBV efficiently inhibited HCV-RNA replication in the ORL8/ORL11 assays, but not in the OR6 assay [22]. This finding led us to clarify the anti-HCV mechanism of RBV [22,23]. Furthermore, we demonstrated that plural assay systems including OR6 and ORL8 were required for the objective evaluation of anti-HCV reagents [24]. In that study, we observed that the antimalarial drug artemisinin possessed weak anti-HCV activity, as reported previously [25].

From these results, we considered that antimalarial drugs might be good candidates for anti-HCV reagents, since the proliferation of both HCV and malaria generally occurs in hepatocytes. We therefore examined the anti-HCV activity of two preclinical antimalarial drugs, N-89 and its derivative water soluble N-251, which were previously discovered by our group as promising antimalarial reagents [26–28]. Here we report that N-89 and N-251 exhibit very fast and potent anti-HCV activities and have promise as potential anti-HCV drugs.

Table 1. Anti-HCV activities of N-89 or N-251 in various HCV drug assay systems.

Cell origin	HuH-7						Li23							
HCV strain	**O**		**1B-4**		**AH1**		**O**		**O**		**1B-4**		**KAH5**	
Assay	OR6		1B-4R		AH1R		ORL8		ORL11		1B-4RL		KAH5RL	
Reagents	9.0[*1]	14[*3]	9.3	22	>0.5	>20	2.3	26	0.56	12	2.4	20	2.5	13
N-89	0.66[*2]		0.42		0.025		0.089		0.045		0.12		0.19	
N-251	3.0	4.4	3.8	3.9	0.49	3.5	1.3	13	1.1	19	1.9	8.3	2.8	10
	0.69		0.98		0.14		0.10		0.059		0.23		0.29	
HCV strain	O						O		O					
Assay	sOR						sORL8		sORL11					
Reagents	1.7	2.9					1.1	9.2	1.7	14				
N-89	0.58						0.12		0.12					
N-251	2.2	3.2					4.1	19	3.1	11				
	0.69						0.22		0.27					

*[1]CC_{50} value (μM),
*[2]EC_{50} value (μM),
*[3]SI value.
doi:10.1371/journal.pone.0072519.t001

Materials and Methods

Cell Culture

RSc and D7 cells were derived from the cell lines HuH-7 and Li23, respectively, were cultured as described previously [20,29]. HuH-7-derived OR6 [13], AH1R [30], and 1B-4R [Ikeda et al., submitted] cells harboring genome-length HCV-RNA and HuH-7-derived polyclonal sOR [31], and RSc-JRN/35B [Ikeda et al., submitted] cells harboring an HCV subgenomic replicon were cultured with medium in the presence of G418 (0.3 mg/ml; Geneticin, Invitrogen, Carlsbad, CA) as described previously [13]. Li23-derived ORL8 [20], ORL11 [20], 1B-4RL [Ikeda et al., submitted], and KAH5RL [Ikeda et al., submitted] cells harboring genome-length HCV-RNA were maintained with medium in the presence of G418 (0.3 mg/ml) as described previously [20]. Li23-derived polyclonal sORL8 and sORL11 cells harboring an HCV replicon, which were established by the transfection of ORN/3-5B/QR,KE,SR RNA into the cured OL8 and OL11 cells, respectively, were also cultured with medium in the presence of G418 (0.3 mg/ml) as described previously [20]. Cured cells, from which the HCV-RNA had been eliminated by IFN treatment, were also maintained with medium in the absence of G418 as described previously [13]. HCV-RNA-replicating cells possess the G418-resistant phenotype because neomycin phosphotransferase as a selective marker was produced by the efficient replication of HCV-RNA. Therefore, when HCV-RNA is excluded from the cells or when its level is decreased, the cells are killed in the presence of G418.

Reagents

N-89 and N-251 were synthesized according to the methods described previously [26–28]. RBV was kindly provided by Yamasa (Chiba, Japan). Human IFN-α and vitamin E (VE) were purchased from Sigma-Aldrich (St. Louis, MO). Cyclosporine A (CsA) was purchased from Tokyo Chemical Industry (Tokyo, Japan). Artemisinin was purchased from Alexis Biochemicals (San Diego, CA).

RL Assay

RL assay was performed as described previously [20,24]. Briefly, the cells were plated onto 24-well plates (2×10^4 cells per well) in triplicate and then treated with each reagent at several concentrations for 72 hrs. After treatment, the cells were subjected to luciferase assay using the RL assay system (Promega, Madison, WI). The experiments were performed at least in triplicate. From the assay results, the 50% effective concentration (EC_{50}) of each reagent was determined.

WST-1 Cell Proliferation Assay

The WST-1 cell proliferation assay was performed as described previously [24]. Briefly, The cells were plated onto 96-well plates (1×10^3 cells per well) in triplicate and then treated with each reagent at several concentrations for 72 hrs. After treatment, the cells were subjected to the WST-1 cell proliferation assay (Takara Bio, Otsu, Japan) according to the manufacturer's protocol. This assay is based on the enzymatic cleavage of the tetrazolium salt WST-1 to formazan by cellular mitochondrial dehydrogenases present in viable cells. Therefore, there are viable cells even if the value of the WST-1 assay becomes zero. The experiments were performed at least in triplicate. From the assay results, the 50% cytotoxic concentration (CC_{50}) of each reagent was determined.

Western Blot Analysis

The preparation of cell lysates, sodium dodecyl sulfate-polyacrylamide gel electrophoresis, and immunoblotting analysis were performed as previously described [32]. The antibodies used in this study were those against HCV Core (CP11; Institute of Immunology, Tokyo, Japan), NS5B (a generous gift from Dr. M. Kohara, Tokyo Metropolitan Institute of Medical Science), and β-actin (AC-15; Sigma-Aldrich) as the control for the amount of protein loaded per lane.

Selective Index (SI)

The SI value of each reagent was determined by dividing the CC_{50} value by the EC_{50} value.

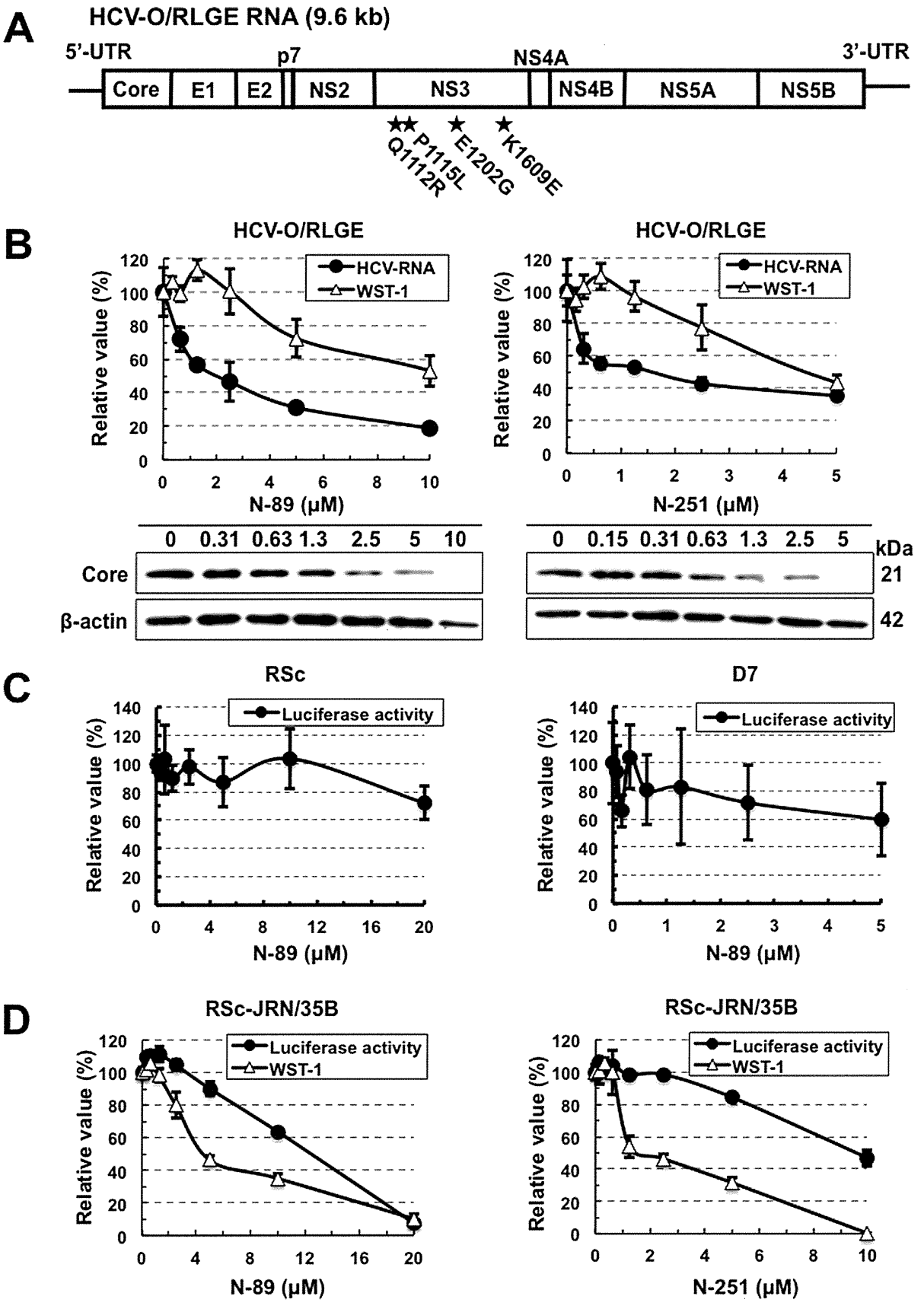
A
HCV-O/RLGE RNA (9.6 kb)
5'-UTR
p7
NS4A
3'-UTR
Core
E1
E2
NS2
NS3
NS4B
NS5A
NS5B
P1115L
Q1112R
E1202G
K1609E
B
HCV-O/RLGE
HCV-O/RLGE
HCV-RNA
WST-1
Relative value (%)
N-89 (μM)
N-251 (μM)
0 0.31 0.63 1.3 2.5 5 10
0 0.15 0.31 0.63 1.3 2.5 5
kDa
Core
β-actin
21
42
C
RSc
D7
Luciferase activity
N-89 (μM)
D
RSc-JRN/35B
RSc-JRN/35B
Luciferase activity
WST-1
N-89 (μM)
N-251 (μM)

Figure 2. Characterization of anti-HCV activities of N-89 and N-251. (A) Schematic gene organization of authentic HCV-RNA (HCV-O/RLGE). The positions of four adaptive mutations - Q1112R, P1115L, E1202G, and K1609E - are indicated by a black star. (B) N-89 and N-251 inhibited authentic HCV-RNA replication. The cells harboring HCV-O/RLGE RNA [19] were treated with N-89 (left panel) and N-251 (right panel) for 72 hrs, followed by real-time LightCycler PCR (black circles in the upper panel) and WST-1 assay (open triangles in the upper panel). The relative value (%) calculated at each point, when the level in non-treated cells was assigned as 100%, is presented here. Data are expressed as the means±standard deviation of triplicate assays. Western blot analysis (lower panels) was performed as described in Fig. 1B. (C) N-89 did not inhibit the HCV-JFH-1 replication. RSc (left panel) and D7 (right panel) cells were inoculated with supernatant from RSc cells replicating JR/C5B/BX-2 [29]. The RL assay was performed as described in Fig. 1B. (D) N-89 (left panel) and N-251 (right panel) did not inhibit the replication of HCV-JFH-1 subgenomic replicon. The RL and WST-1 assays were performed as described in Fig. 1B.
doi:10.1371/journal.pone.0072519.g002

Quantitative RT-PCR Analysis

The RNAs from HCV-RNA replicating cell lines were prepared with an RNeasy extraction kit (Qiagen). The quantitative RT-PCR analysis for HCV-RNA was performed using a real-time LightCycler PCR (Roche Diagnostics, Basel, Switzerland) as described previously [13,20].

HCV Infection

HCV infection was performed as described previously [29]. RSc and D7 cells were inoculated with supernatant from RSc cells replicating JR/C5B/BX-2 [29].

Statistical Analysis

Determination of the significance of differences among groups was assessed using the Student's *t*-test. $P<0.05$ was considered significant.

Results

Preclinical Antimalarial Drugs, N-89 and N-251, Showed Potent Anti-HCV Activities in Both HuH-7- and Li23-derived Genome-length HCV-RNA-replicating Cells

Recently we demonstrated that plural HCV assay systems developed using both HuH-7 and Li23 cell lines or HCV strains belonging to genotype 1b are required for the objective evaluation of anti-HCV candidates [24]. In the present work, we used our previously developed HCV assay systems to evaluate preclinical antimalarial drugs (N-89 and N-251). N-89 (1,2,6,7-Tetraoxaspiro[7.11]nonadecane) is a chemically synthesized endoperoxide compound (Fig. 1A) with potent antimalarial activity against *Plasmodium falciparum in vitro* and *Plasmodium berghei in vivo*, and it shows low levels of cytotoxicity in mice and rats (50% lethal dose: >2000 mg/kg) [26,33,34]. N-251 (6-(1,2,6,7-tetraoxaspiro[7.11]-nonadec-4-yl)hexan-1-ol), which bears a functional side chain hydroxyl group that allows derivatization, is synthesized by replacing the hydrogen at C-4 of N-89 with hexanol (Fig. 1A), and it is as potent as N-89 against malaria parasites [27,28]. We first evaluated the anti-HCV activities of N-89 and N-251 using HuH-7-derived OR6 and Li23-derived ORL8 and ORL11 assay systems. The results revealed that both N-89 and N-251 possessed strong anti-HCV activities (Fig. 1B and C). The EC_{50} and SI values of N-89 in each assay were calculated (EC_{50} 0.66 μM, SI 14 in OR6 assay; EC_{50} 0.089 μM, SI 26 in ORL8 assay; EC_{50} 0.045 μM, SI 12 in ORL11 assay) (Table 1), and the anti-HCV activity of N-251 was found to be as potent as that of N-89 (Table 1). The anti-HCV activities of N-89 and N-251 were confirmed by Western blot analysis of HCV Core (Fig. 1B and C). To further evaluate the activities of N-89 and N-251, as additional assay systems, we used HuH-7-derived 1B-4R (1B-4 strain [31] of

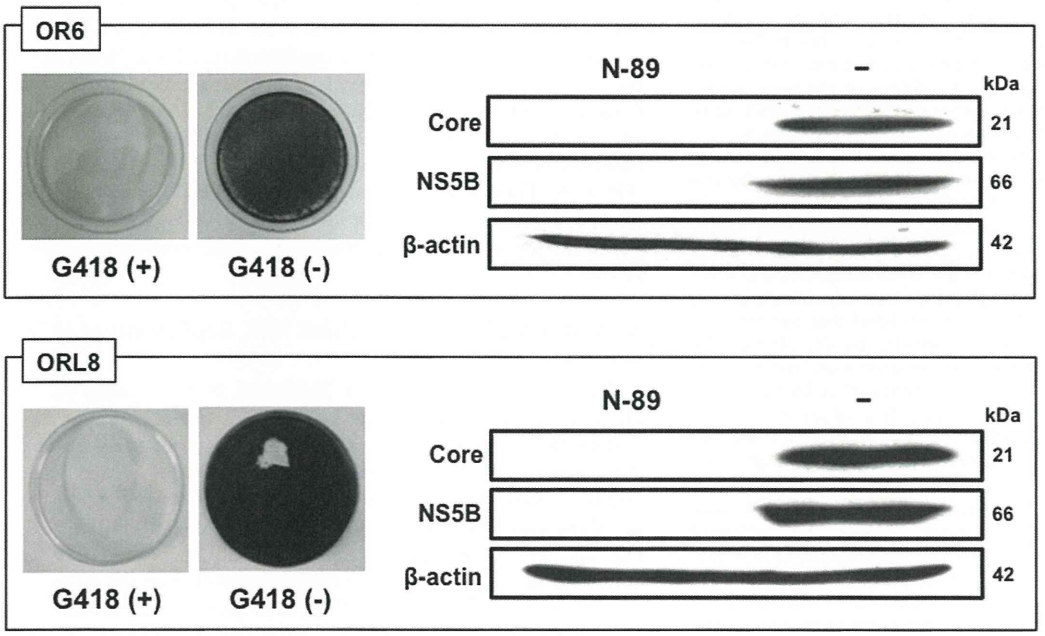

Figure 3. OR6 and ORL8 cells were cured by treatment with only N-89. The treated cells were divided into two plates with or without G418, and then cultured for 2 weeks. The left panels show the cells stained with Coomassie brilliant blue. The right panels show the results of Western blot analysis of the treated and non-treated cells for HCV proteins. Western blot analysis was performed as described in Fig. 1B.
doi:10.1371/journal.pone.0072519.g003

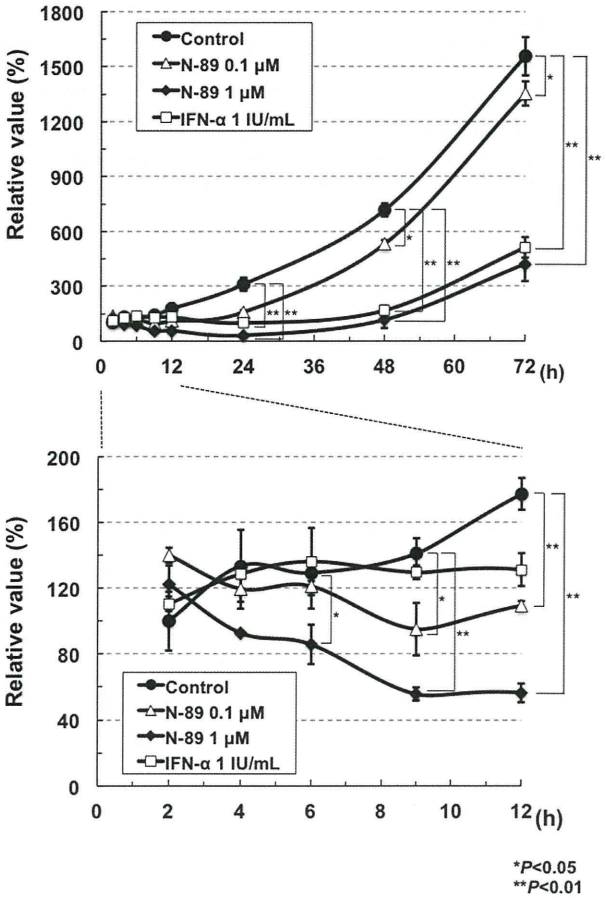

Figure 4. The anti-HCV action of N-89 was faster than that of IFN-α. The ORL8 cells were treated with N-89 or IFN-α, and then RL assays were performed at 2 to 72 hrs after the treatment. The relative value (%) calculated at each time point, when the luciferase activity of non-treated cells at 24 hrs was assigned as 100%, is shown. Data are expressed as the means±standard deviation of triplicate assays. The data within 12 hrs after the treatment are shown in the lower panel. *$P<0.05$; **$P<0.01$.**The** Anti-**HCV** Activities **of N-89 and N-251 were** Completely Canceled **by VE**We previously reported that the antioxidant VE canceled the anti-HCV activities of CsA and three nutrients (β-carotene, vitamin D_2, and linoleic acid) [37], and demonstrated that the oxidative stress induced by these anti-HCV reagents caused anti-HCV status via activation of the extracellular signal-regulated kinase signaling pathway [38]. To evaluate this possibility, we examined the effect of VE on N-89 at the EC_{90} level in the ORL8 assay. CsA and IFN-α were also used as a positive and a negative control, respectively, on the effect of VE in the ORL8 assay. The results revealed that the anti-HCV activities of N-89 and CsA were largely canceled by VE, whereas the activity of IFN-α was not canceled (Fig. 5A). We normalized these results by dividing the RL value obtained in the presence of VE by that in the absence of VE as described previously [22,37]. The values of N-89 and CsA were 16 and 34, respectively, whereas the value (3.2) of IFN-α was almost the same as that (3.0) of the control (Fig. 5B). Similar results were obtained by using N-251 (Fig. 5C and D). The values of N-251, CsA, and IFN-α were 13, 19, and 4.3, respectively, in comparison with the value (2.3) of the control (Fig. 5D). These results suggest that the induction of oxidative stress is associated with the anti-HCV activity of N-89 or N-251. However, an antimalarial drug, artemisinin, was hardly influenced by co-treatment with VE (Fig. 5E). The value (1.9) of artemisinin was almost the same as that (3.5 or 2.5) of IFN-α or the control, respectively (Fig. 5F). These results were also confirmed by Western blot analysis of HCV Core (Fig. 5G). Therefore, our results suggest that the anti-HCV mechanism of artemisinin is not associated with the induction of oxidative stress, and is distinct from that of N-89 or N-251.
doi:10.1371/journal.pone.0072519.g004

genotype 1b derived from an HCV-positive healthy carrier) [Ikeda et al., submitted] and AH1R (an AH1 strain [35] of genotype 1b derived from a patient with acute hepatitis C) [30], and Li23-derived 1B-4RL (1B-4 strain [31]) and KAH5RL (KAH5 strain [31] of genotype 1b derived from a patient with acute hepatitis C) [Ikeda et al., submitted]. These assays also showed that N-89 and N-251 possessed potent anti-HCV activities (Fig. S1A–D and Table 1). It was noteworthy that N-89 exhibited the strongest anti-HCV activity (EC_{50} 0.025 μM; SI >20) in the AH1R assay (Fig. S1A and Table 1). These results suggest that the anti-HCV activity of N-89 or N-251 is not influenced by the cell line or HCV strain. We next examined the activities of N-89 and N-251 using polyclonal cell-based assay systems (HuH-7-derived sOR [31], Li23-derived sORL8 and sORL11 [22]) that facilitate the monitoring replication of HCV subgenomic replicon RNA. These assays also showed that N-89 and N-251 possessed anti-HCV activity with EC_{50} values of less than 1 μM (Fig. S1E-G and Table 1). Taken together, these results indicate that the anti-HCV activities of N-89 and N-251 are not dependent on the specific cloned cell line or HCV structural proteins.

N-89 and N-251 Inhibited Authentic HCV-RNA Replication

The genome-length HCV-RNA used in the assay systems described above contains three non-natural elements: RL, neomycin phosphotransferase, and an internal ribosomal entry site of encephalomyocarditis virus. To exclude the possibility that the anti-HCV activity of N-89 or N-251 was due to the inhibition of these three exogenous elements, we examined the anti-HCV activities of N-89 and N-251 using the authentic 9.6 kb HCV-RNA-replicating HCV-O/RLGE cells [19], which were developed by the introduction of *in vitro* synthesized HCV-O/RLGE RNA (Fig. 2A) into OR6c cured cells. We could demonstrate by quantitative RT-PCR and Western blot analyses that N-89 and N-251 at the expected concentrations efficiently prevented HCV-RNA replication and HCV Core expression in HCV-O/RLGE cells in a dose-dependent manner, respectively (Fig. 2B). The EC_{50} and SI values of N-89 and N-251 in this assay were calculated as follows each: EC_{50} 2.0 μM and SI >5.0 in N-89; EC_{50} 1.6 μM and SI 2.8 in N-251. To further confirm that N-89 or N-251 does not inhibit the RL activity, we examined the direct effect of each reagent by adding it along with substrate to the cell lysate in the RL assay. No suppressive effects by N-89 and N-251 were observed in either the OR6 assay (Fig. S2A) or the ORL8 assay (Fig. S2B). These results indicate that the anti-HCV activities of N-89 and N-251 were due to the inhibition of HCV-RNA itself, but not to exogenous elements contained in the genome-length HCV-RNA.

N-89 and N-251 did not Inhibit RNA Replication of HCV-JFH-1 Strain

We next examined whether N-89 and N-251 worked in an HCV production system using HCV-JFH-1 strain (genotype 2a). Unexpectedly, the results using the JFH-1 reporter assay systems [29], which were recently developed using HuH-7-derived RSc and Li23-derived D7 cells, revealed that both N-89 and N-251 did not show anti-HCV activity for the HCV-JFH-1 strain (Fig. 2C, Fig. S3). To clarify whether anti-HCV activity depends on the difference of genotype or assay model, we evaluated the activities of N-89 and N-251 using RSc-JRN/35B [Ikeda et al., submitted] cells harboring a subgenomic HCV-JFH-1 replicon as an additional assay. The results revealed that N-89 and N-251 did not show any anti-HCV activities in this assay system either (Fig. 2D). Although the relative value of WST-1 almost became zero when RSc-JRN/35B cells were treated with 10 μM of N-251,

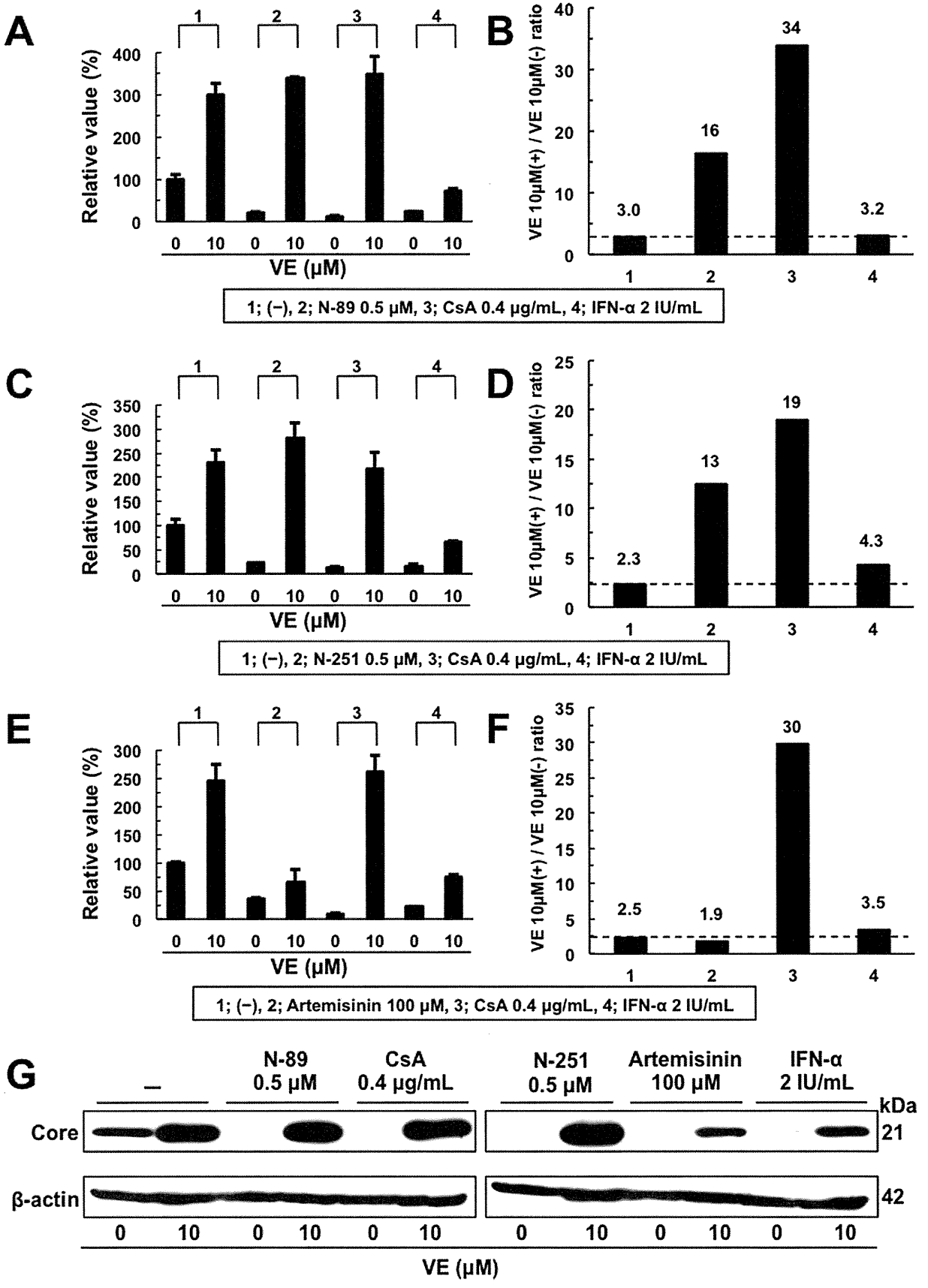
A
Relative value (%)
VE (μM)
1; (−), 2; N-89 0.5 μM, 3; CsA 0.4 μg/mL, 4; IFN-α 2 IU/mL
B
VE 10μM(+) / VE 10μM(-) ratio
3.0
16
34
3.2
C
Relative value (%)
VE (μM)
1; (−), 2; N-251 0.5 μM, 3; CsA 0.4 μg/mL, 4; IFN-α 2 IU/mL
D
VE 10μM(+) / VE 10μM(-) ratio
2.3
13
19
4.3
E
Relative value (%)
VE (μM)
1; (−), 2; Artemisinin 100 μM, 3; CsA 0.4 μg/mL, 4; IFN-α 2 IU/mL
F
VE 10μM(+) / VE 10μM(-) ratio
2.5
1.9
30
3.5
G
—
N-89 0.5 μM
CsA 0.4 μg/mL
N-251 0.5 μM
Artemisinin 100 μM
IFN-α 2 IU/mL
kDa
Core
21
β-actin
42
VE (μM)